

**JIMMA UNIVERSITY**  
**SCHOOL OF GRADUATE STUDIES**  
**COLLEGE OF NATURAL SCIENCES**  
**DEPARTMENT OF CHEMISTRY**



**SYNTHESIS AND CHARACTERIZATION OF SILVER DOPED  
MANGANESE OXIDE NANOCOMPOSITES USING *Croton Macrostachyus*  
LEAF EXTRACT AND EVALUATION OF ITS ANTIMICROBIAL  
ACTIVITY**

**BY: MEGERSA SOBOKA**

**ADVISOR: GUTA GONFA (Ph. D)**

**CO-ADVISOR: AHMED AWOL (Asst.prof)**

**APRIL, 2022**

**JIMMA, ETHIOPIA**

SYNTHESIS AND CHARACTERIZATION OF SILVER DOPED  
MANGANESE OXIDE NANOCOMPOSITES USING *Croton Macrostachyus* LEAF  
EXTRACT AND EVALUATION OF ITS ANTIMICROBIAL ACTIVITY

A THESIS PAPER SUBMITTED TO SCHOOL OF GRADUTE STUDIES, JIMMA  
UNIVERSITY IN PARTIAL FULFILMENT OF THE REQUIRMENTS FOR THE DEGREE  
OF MASTERS OF SCIENCE IN CHEMISTRY (INORGANIC CHEMISTRY)

By:  
MEGERSA SOBOKA

ADIVISOR: GUTA GONFA (Ph. D)

CO-ADVISOR: AHMED AWOL (Asst.prof)

APRIL, 2022

JIMMA, ETHIOPIA

## APPROVAL OF BOARD OF EXAMINERS

We, the undersigned, members of the Board of Examiners of the final open defense by Megersa Soboka have read and evaluated his thesis entitled “**synthesis and characterization of silver doped manganese oxide nanocomposites using *C. macrostachyus* leaf extract and evaluation of its antimicrobial activity**” and examined the candidate. This is, therefore, to certify that the thesis has been accepted in partial fulfillment of the requirement of the Degree of masters in chemistry

Dr. Guta Gonfa

Advisor

\_\_\_\_\_

Signature

\_\_\_\_\_

Date

Mr. Gebru G/Tsedik

Chairperson

\_\_\_\_\_

Signature

\_\_\_\_\_

Date

Mr. Kirubel Teshome

Internal Examiner

\_\_\_\_\_

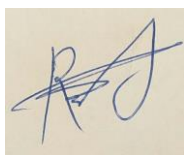
Signature

\_\_\_\_\_

Date

Dr. Raji Feyisa

External Examiner



\_\_\_\_\_

Signature

14/04/2022

Date

## **DECLARATION**

I hereby declare that this MSc Thesis is my original work and has not been presented for a degree in any other university, and all sources of material used for this thesis have been duly acknowledged.

Name: \_\_\_\_\_

Signature: \_\_\_\_\_

This MSc Thesis has been submitted for examination with my approval as thesis advisor

Name: \_\_\_\_\_

Signature: \_\_\_\_\_

Date of submission \_\_\_\_\_

# TABLE OF CONTENTS

Contents	Pages
LIST OF TABLES .....	iv
LIST OF FIGURES .....	v
LIST OF APPENDIXES.....	vi
ABBREVIATIONS AND ACRONYMS .....	vii
ACKNOWLEDGEMENT .....	viii
ABSTRACT.....	ix
1. INTRODUCTION .....	1
1.1 Background of the Study.....	1
1.2 Statement of the Problem .....	3
1.3 Objectives.....	4
1.3.1 General Objective .....	4
1.3.2 Specific Objectives .....	4
1.4 Significance of the Study .....	4
2. LITERATURE REVIEW.....	5
2.1 Nanomaterials.....	5
2.2 Methods Synthesis of Nanomaterials.....	5
2.2.1 Synthesis of Nanoparticles.....	6
2.2.2 Green synthesis .....	7
2.2.3 Synthesis of Nanoparticles by Using Plant.....	7
2.3 Application of Nanomaterials and Nanotechnology .....	9
2.4 Medicinal Value of <i>Croton Macrostachyus</i> .....	10
2.5 Characterization Technique for Metal and Metal Oxide Nanoparticles .....	11
2.5.1 UV-Visible Spectroscopy .....	11
2.5.2 Fourier Transformation Infrared (FT-IR) Spectroscopy.....	11
2.5.3 X-ray diffraction (XRD) .....	12
2.5.4 Scanning Electron Microscopy (SEM) .....	12
2.6 Biological assay.....	13
2.6.1 Antimicrobial resistance .....	13

3.	MATERIALS AND METHODS .....	15
3.1	Chemicals and Materials .....	15
3.2	Apparatus .....	15
3.3	Instruments .....	15
3.4	Sample Collection and Preparation .....	15
3.5	Preliminary Phytochemical Screening .....	16
3.5.1	Test for Phenols .....	16
3.5.2	Test for Flavonoids .....	16
3.5.3	Test for Alkaloids .....	16
3.6	Parameters Optimization for the synthesis of MnO NPs .....	16
3.6.1	pH optimization .....	16
3.6.2	Plant Extract Volume .....	16
3.6.3	Concentration of Precursor .....	17
3.7	Synthesis MnO NPs .....	17
3.7.1	Synthesis of Ag-MnO Nanocomposite .....	17
3.8	Characterization Technique for Metal and Metal Oxide Nanoparticles .....	18
3.8.1	UV-Vis Spectroscopy Studies.....	18
3.8.2	Fourier Transform Infrared (FT-IR) Spectroscopy Studies .....	18
3.8.3	X-ray diffraction (XRD) Studies .....	18
3.8.4	Scanning Electron Microscopy (SEM) Studies .....	18
3.9	Electrochemical Studies of MnO NPs.....	19
3.10	Antimicrobial activity .....	19
3.11	Preparations of Test Solution .....	20
4.	RESULTS AND DISCUSSION.....	21
4.1	Phytochemical Analysis of <i>Croton Macrostachyus</i> Leaves Extract .....	21
4.2	Synthesis Manganese Oxide Nanoparticles .....	21
4.3	Optimization of parameters during synthesis of MnO NPs .....	21
4.3.1	Effect of pH.....	22
4.3.2	Plant Extract Volume.....	23
4.3.3	Concentration of KMnO <sub>4</sub> Optimization.....	24
4.4	UV–Visible Spectroscopy Analysis .....	25

4.5	FT-IR Analysis of Synthesized MnO NPs from <i>Croton Macrostachyus</i> .....	26
4.6	XRD Analysis of Synthesized MnO NPs from <i>C. Macrostachyus</i> .....	27
4.7	Synthesis of Ag-Doped MnO Nanocomposite.....	28
4.7.1	UV-Vis Analysis of Synthesized Ag-MnO NCs from <i>C. Macrostachyus</i> .....	28
4.7.2	FT-IR Analysis of Synthesized Ag-MnO NCs from <i>C. Macrostachyus</i> .....	30
4.7.3	XRD Analysis of Synthesized Ag-MnO NCs from <i>C. Macrostachyus</i> .....	31
4.8	Scanning Electron Microscopy (SEM) Analysis .....	32
4.9	Electrochemical Analysis of Synthesized MnO NPs .....	32
4.10	Antimicrobial Activity Analysis .....	33
5.	CONCLUSION AND RECOMMENDATIONS .....	36
5.1	Conclusion.....	36
5.2	Recommendations .....	37
	REFERENCES .....	38
	APPENDIXES .....	46

## LIST OF TABLES

Table 1 Phytochemical components of <i>Croton Macrostachyus</i> plant extract .....	21
Table 2 Optimization of pH .....	22
Table 3 The optimization of plant extract volume.....	23
Table 4 The KMnO <sub>4</sub> (precursor) concentration optimization.....	24
Table 5 Comparison of size of MnO NP with different works.....	27
Table 6 Synthesized MnO NPs and Ag-MnO NCs from <i>C. macrostachyus</i> leaf extract and their antibacterial and fungal activity.....	34



## LIST OF FIGURES

Figure 1 Nanoparticles synthesis via biological and physicochemical approaches.....	6
Figure 2 Environment-friendly and cheap route for the green synthesis of nanoparticles using plants extract. ....	8
Figure 3 Application of nanotechnology in science and environmental science.....	9
Figure 4 <i>Croton macrostachyus</i> plant.....	10
Figure 5 some use <i>Croton Macrostachyus</i> plant.....	11
Figure 6 UV-Visible spectra of the optimization pH of Manganese Oxide Nanoparticles. ....	23
Figure 7 UV-Vis of MnO NPs of the optimization of plant extract volume. ....	24
Figure 8 UV – Vis spectra of MnO NPs the optimization of precursor concentration.....	25
Figure 9 FT-IR spectra of MnO NPs synthesized from <i>C. macrostachyus</i> leaf extract .....	26
Figure 10 XRD pattern of synthesized undoped MnO NPs.....	28
Figure 11 UV-Visible spectrum of Ag-MnO NCs synthesized from <i>C. macrostachyus</i> leaf extract.....	29
Figure 12 UV- Vis spectra of A) MnO NPs and Ag-MnO NPs. ....	29
Figure13 FT-IR spectra of synthesized MnO NPs & Ag-MnO NCs using <i>C. macrostachyus</i> leaf extract.....	30
Figure 14 XRD pattern obtained for <i>C. macrostachyus</i> synthesized Ag-MnO NCs.....	31
Figure 15 SEM image of MnO NPs and Ag-MnO NCs synthesized from <i>C. macrostachyus</i> leaf extract.....	32
Figure 16 Cyclic Voltammetry analysis of MnO NPs /gold electrode of oxidized and reduced on phosphate buffer solution.....	33
Figure 17 The antimicrobial test of leaf extract, MnO NPs and Ag-MnO NCs. ....	35

## LIST OF APPENDIXES

Appendix 1 schematic diagram show the preparation of <i>croton macrostachyus</i> leaf extract. ....	46
Appendix 2 Schematic diagram show the formation of manganese oxide nanoparticles.....	47
Appendix 3 Phytochemical screening of phenols, flavonoids and alkaloids.....	48

## ABBREVIATIONS AND ACRONYMS

Ag	Silver
<i>B. cereus</i>	<i>Bacillus cereus</i>
<i>C. albicans</i>	<i>Candida albicans</i>
<i>C. macrostachyus</i>	<i>Croton macrostachyus</i>
<i>C. pepo</i>	<i>Cucurbita pepo</i>
CV	cyclic voltammetry
DMSO	Dimethylsulfoxide
DPV	Differential pulse voltammetry
D W	Distilled water
<i>E. coli</i>	<i>Escherichia coli</i>
FT-IR	Fourier transform infrared
MnO	Manganese oxide
MnO NPs	Manganese oxide nanoparticles
NCs	Nanocomposites
NPs	Nanoparticles
NIZ	No inhibition zone
<i>S. aureus</i>	<i>Staphylococcus aureus</i>
<i>S. typhi</i>	<i>Salmonella typhi</i>
SEM	Scanning electron microscopy
UV-Vis	Ultraviolet-Visible Spectroscopy
XRD	X-ray diffraction

## **ACKNOWLEDGEMENT**

First, I would like to praise my Almighty God for giving me health, knowledge and strength during this work and for his perfect protection and guidance of my life. Next, I would like to thank my advisors Dr. Guta Gonfa and Ahmed Awol (Asst.prof) for their encouragements, supports and continual guidance and understandings throughout my study. I would also thank Department of Chemistry, Jimma University for the facility support, learning environment and internet access.

I would like to extend my great thanks to my parents for their financial support and encouragement.

Lastly, I would also like to expand my deepest gratitude to all those who have directly and indirectly guided me in writing this thesis paper.

## ABSTRACT

Recently, green technology through biosynthesis method has drawn great attention compared to the physical and chemical methods. NPs produced by plant extracts are more stable and biocompatible in comparison with those produced by other methods. Physical and chemical method used, hence green synthesis is inexpensive, low cost and environmentally friendly. This research focused on the synthesis of MnO NPs and Ag-MnO NCs using *C. macrostachyus* leaf extracts and evaluation of their antimicrobial activities. The synthesized nanoparticles were characterized by using UV-Vis, FT-IR, XRD, SEM, and CV. From UV-Vis absorption spectrum the peaks of MnO NPs and Ag-MnO NCs were detected at 230 and 232 nm. The FT-IR spectroscopy revealed the presence of secondary metabolites like phenols, flavonoids, alkaloids, and others in the synthesized nanoparticles and nanocomposites. The crystalline structure were examined the XRD technique, the results indicated that the synthesized NPs had amorphous nature and Ag-doped has 25.54 nm crystalline size. The SEM images of MnO NPs and Ag-MnO NCs indicate formation of pentagon shaped MnO NPs the morphology polymorphic and slightly the agglomerate size which changed to rod-like shape on doping. The reduction of metal ion during stabilization by phytochemicals while forming MnO NPs and Ag-MnO NCs were characterized by CV. The antimicrobial activity of the plant extract and the synthesized NPs was determined by measuring the zone of inhibition. The synthesized Ag-MnO NCS exhibits activity against two gram positive (*S. aureus* and *B.cereus*) and two gram negative (*E. coli* and *S. typhi*) bacterial as well as fungal (*candida albicans*) test. Therefore, the current study reveals a convenient utilization of *Croton macrostachyus* extract as a reducing agent for the successful synthesis of Ag-MnO NCs through a green synthesis method to obtain significantly active antimicrobial material.

**Keywords:** *Croton macrostachyus*, MnO NPs, Ag-MnO NCs, antimicrobial activities, Green synthesis

# 1. INTRODUCTION

## 1.1 Background of the Study

Nanoparticles are wide class of materials that include particulate substances, which have one dimension less than 100 nm at least [1]. Nanoparticles are very important in developing sustainable technologies for the future, for humanity and the environment.

Medicinal Plant extracts are used for the metal ions bioreduction to form nanoparticles. It has been demonstrated that plant metabolites like sugars, terpenoids, polyphenols, alkaloids, phenolic acids, and proteins play an important role in metal ions reduction into nanoparticles and in supporting their subsequent stability [2]. Plants are a rich source of bioactive chemicals with variety of biological activities [3]. Plant assisted synthesis of nanoparticles have captured a considerable attractive interest in the arena of modern nano-science and technology because of its flexibility, biocompatibility and eco-friendly nature [4]. Plant materials have been used for synthesis of different types of nanoparticles such as gold, silver, platinum and copper.

Different physical and chemical approaches like microwave irradiation, thermal decomposition, sol gel, colloidal thermal synthesis, sonochemical, hydrothermal, and quick precipitation have been employed for the synthesis of MnO NPs and Ag-MnO MCs with desired morphologies. However, these methods require labor-intensiveness, energy, intensive routes, expensive and hazardous chemicals [5]. Hence, simple, low cost, and green synthesis method for nanoparticles is highly required.

Synthesis of Nanoparticles by plants is a green chemistry approach that interconnects nanotechnology and plant biotechnology [6]. From environmental point of view plant extracts used reduction methods can be considered as more effective green approaches for synthesizing metal nanoparticles, because of employing plants towards synthesis of nanoparticles are emerging as advantageous compared to microbes with the presence of broad variability of bio-molecules in plants can act as capping and reducing agents [7].

*C. macrostachyus* is commonly known as; rush foil (English), Bakkaniisa (Afan Oromo) and Bisana (Amharic). It belongs to the Euphorbiaceae with 300 genera and 8,000- 10,000 species and

most abundant plant in the tropics [8, 9]. It is native to Ethiopia, Eretria, Kenya, Tanzania, Uganda and Nigeria which is a medium-sized deciduous tree of East Africa particularly wide spread between 200-2500. In mountainous forests and savannah of the tropical regions and ever green bush land areas that receive between 700-701, 200 mm rainfall annually [10,11,12]. The name of Croton comes from a Greek word ‘Kroton’ which means ticks, because of the seeds’ resemblance to ticks, the specific name “macrostachyus” is a contraction of two words, the Greek word “macro” meaning large and “stachyus” relating to the spike, hence, a species characterized by large spikes [13]. *C. macrostachyus* is regarded as a multipurpose tree by subsistence farmers in Ethiopia, Kenya, and Tanzania and the species has potential in playing an important role in the primary healthcare. The bark, fruits, leaves, roots, and seeds of *C. macrostachyus* are reported to possess diverse medicinal properties and *C. macrostachyus* is used as herbal medicine for at least 61 human and 20 animal diseases and ailments. In the distribution area there is a high degree of medicinal use consensus for bleeding, blood clotting, cancer, constipation, diarrhea, epilepsy, malaria, pneumonia, purgative, ringworm, skin diseases or infections, stomach ache, typhoid, worm expulsion, and wounds [14, 15].

Nowadays, nanoscale antimicrobial agents and nanosized carriers for antibiotics delivery have been developed and they have proven their effectiveness for treating infectious diseases in vitro and animal models MnO nanoparticle is known for its antimicrobial activity against various bacterial pathogens. The green synthesis of Manganese oxide nanoparticles (MnO NPs) has been reported from *Syzygium aromaticum* i.e. clove extract to be applied as a stabilizing as well as reducing agent and the resulting nanoparticles was applied towards p-Nitrophenol (PNP) sensing[16]. Manganese oxides can be applied in catalysts, molecular sieves, ion-sieves, batteries, magnetic material as well as other applications such as water treatment, imaging contrast agents due to their excellent physiochemical properties [17]. MnO is also one of the most important materials and a number of researchers pay attention to influence of MnO addition on electromagnetic properties of ferrite materials. Various approaches have been developed to prepare nanoscale MnO such as self-reacting micro emulsion, preparation, room solid reactions, sonochemical and hydrothermal methods [18, 19]. Recently, there work done on synthesis of Ag-doped MnO NCs by *C. Pepo* plant for catalytic activity [20]. Hence, there is no report on synthesis of MnO NPs and Ag-doped MnO NCs by mediation of *Croton macrostachyus* leaf extracts. The

main objective of this work is synthesis of MnO NPs and Ag-doped MnO NCs by using *Croton macrostachyus* leaf extracts.

## 1.2 Statement of the Problem

Traditionally, people have used different plants to treat different diseases without detailed scientific information. *C. macrostachyus* is one of the famous plants traditionally used as medicinal values. The biological activity of these plants can be further enhanced if supported by metal / metal oxide nanoparticles that helping penetrating to the cells of the pathogen. The physical and chemical methods for synthesizing metal oxide nanoparticles are expensive and not environmentally friendly. As a result, metal oxide nanoparticles synthesized from plant leaf extracts impose limited environmental hazards and are relatively biocompatible, chemically and physical method to produce environmentally friendly nanoparticles. *Vernonia amygdalina*, *Kalopanax pictus*, *C. pepo* Plant extracts leaves contain phytochemicals, which can act as reducing agents, capping agents and stabilizers in the process of NPs synthesis [22-24]. However, this study aimed to synthesize MnO NPs and Ag-MnO NCs supported with *C. macrostachyus* leaf extract and evaluate their antimicrobial activity. Additionally, there is no reports on the synthesis of MnO NPs and Ag-MnO NCs using *C. macrostachyus* leaf extracts.

This study may address the following questions;

- Is *Croton Macrostachyus* leave extract acted as stabilizing and capping agent for the synthesis of MnO NPs and Ag-MnO NCs?
- Does Ag-MnO NCs show more antimicrobial activity than MnO NPs?
- Does the synthesized nanoparticles show enhanced activity than that of plant extract?



## **1.3 Objectives**

### **1.3.1 General Objective**

To synthesize and characterize MnO NPs and Ag-MnO NCs using leaf extract of *Croton macrostachyus* and evaluation of their antimicrobial activity.

### **1.3.2 Specific Objectives**

- To prepare *Croton macrostachyus* leaf extract.
- To synthesize MnO NPs and Ag-MnO NCs using *Croton macrostachyus* aqueous leaf extract.
- To characterize MnO NPs and Ag-MnO NCs using UV-Vis, FT-IR, XRD, SEM and CV.
- To evaluate the antibacterial and antifungal activities of plant extract, MnO NPs and Ag-MnO NCs.

## **1.4 Significance of the Study**

The findings of this research was used to-

- The obtained product's applications for antimicrobial activities may be scaled up to palate or clinical test for scaling-up the application tests.
- Setting the ground for further investigation of chemical and health aspects of MnO NPs and Ag-MnO NCs.
- The research out manuscript may serve as a reference materials for different stakeholders for further work on this area

## 2. LITERATURE REVIEW

### 2.1 Nanomaterials

Nanotechnology is a field of science and technology, which deals with production, manipulation and use of materials carrying in nanometers. NPs are wide class of materials that include particulate substances, which have one dimension less than 100 nm at least [25]. Nano materials having a length scale less than 100 nm have received increasing interest owing not only to their fundamental scientific significance but also to the potential applications that derive from their fascinating electrical, magnetic, and catalytic properties [26]. Compared to bulk active electrode materials, the corresponding nanomaterial possess more excellent electrochemical activity, such as higher capacities, larger surface areas, and lower current densities, thereby; nanomaterial have wildly potential application in electrochemistry field. Manganese oxides, including MnO, MnO<sub>2</sub>, and Mn<sub>3</sub>O<sub>4</sub>, are intriguing composites and have been used in wastewater treatment, catalysis, sensors, supercapacitors and alkaline and rechargeable batteries [27-31]. Particularly, MnO and MnO<sub>2</sub> nanomaterial have attracted great interest as anode materials in lithium-ion batteries (LIBs) for their high theoretical capacity, low cost, environmental benignity, and special properties [32-34].

### 2.2 Methods Synthesis of Nanomaterials

Various methods can be employed for the synthesis of NPs, but these methods are broadly divided into two main classes. i.e. (1) Bottom-up approach and (2) Top-down approach [35] as shown in (Fig. 1). These approaches further divide into various subclasses based on the operation, reaction condition and adopted protocols.

#### A. Top-down Approach

In this method, destructive approach is employed. Starting from larger molecule, which decomposed into smaller units and then these units are converted into suitable NPs. Examples of this method are grinding/milling, chemical vapour deposition (CVD), physical vapour deposition (PVD) and other decomposition techniques [35]. The principle behind the top-down approach is to take a bulk piece of the material and then modify it into the wanted nanostructure and subsequent stabilization of the resulting nanosized metal nanoparticles by the addition of colloidal protecting agents. Cutting, grinding and etching are typical fabrication techniques, which have been

developed to work on the nano scale. The sizes of the nanostructures which can be produced with top-down techniques are between 10 to 100 nm [36].

## B. Bottom-up Approach

This approach is employed in reverse as NPs are formed from relatively simpler substances, therefore this approach is also called building up approach. Examples of this case are sedimentation and reduction techniques. It includes sol-gel, green synthesis, spinning, and biochemical synthesis [35]. This refers to the construction of a structure atom by atom, molecule-by molecule or cluster by cluster. Colloidal dispersion used in the synthesis of nanoparticles is a good example of a bottom-up approach. An advantage of the bottom-up approach is the better possibilities to obtain nanostructures with less defects and more homogeneous chemical compositions [36].

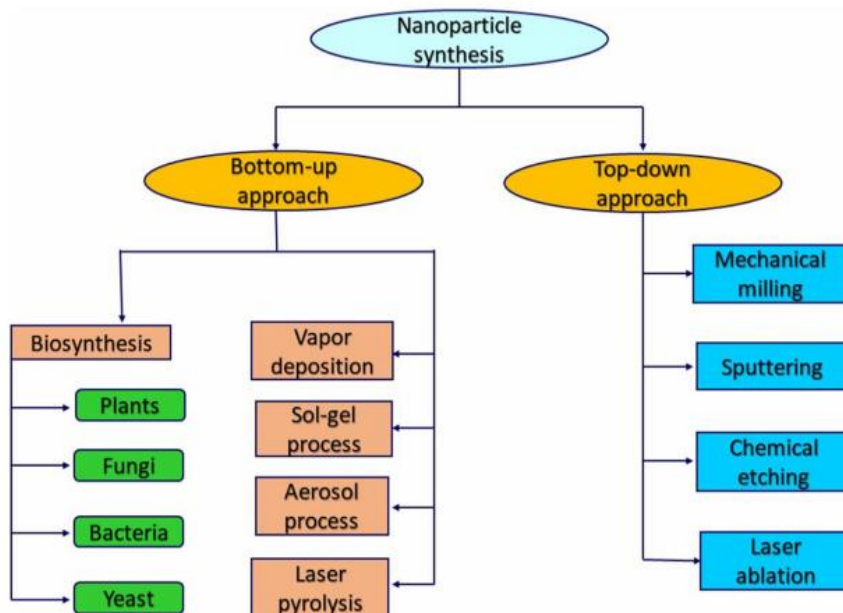


**Figure 1** Nanoparticles synthesis via biological and physicochemical approaches.

### 2.2.1 Synthesis of Nanoparticles

Synthesis of NPs is to reduce the metal ions in the solution using a reducing agent. NPs are highly reactive due to their high surface energy, and they are aggregated without protection. Lots of natural and synthetic polymers are being used as stabilizing agents to prevent metal NPs from

sedimentation, agglomeration, and oxidation. Manganese NPs (MnO NPs) are being widely used in wastewater treatment, rechargeable batteries, and sensors of p-nitrophenol, molecular sieve, magnetic materials and catalysis [37]. NPs can be synthesized through various methods. Typical methods for synthesis of NPs apply toxic chemicals as reducing agents or as stabilizing agents to preclude NPs from agglomeration. The noble therapeutic applications of NP oblige using environmentally friendly methods. Using enzymes, plant extracts and microorganisms are the biological methods of synthesis of NPs.

### **2.2.2 Green synthesis**

Green synthesis is a plant mediated synthesis of metal nanoparticles it is simple, easily available, fast and ecofriendly among all the synthesis methods. The bio molecules which are present in the plant materials can increase the rate of nano synthesis or the stability of the product. In this method first of all collect plant extract from boiling leaves of regarding plant in di ionized water. Further use this extract with precursor and form nanoparticles. Plant materials have an important role in surface morphology and size of the metals. Extracts from plants may act both as capping and reducing agent in nanoparticle synthesis. But the particles formed by this method may have large sizes [38].

The use of plants or plant extracts, which act as reducing and capping or stabilizing agents for NP synthesis, is more useful over other biosynthesis procedures. This occurs because in this technique, no need cell culturing and cell maintenance [39].

Bacteria produce metal/metal oxide NPs in nanoscale with excellent morphology by extra-or intracellular methods [40]. The various types of bacteria generally involve an intracellular method, where by the bacterial cell filtrate is treated with a metal solution and maintained in an orbital shaker in the dark at room temperature (RT) and adequate pressure conditions [41]. The use of fungi to produce different NPs has received great interest as they offer certain benefits over bacteria [42].

### **2.2.3 Synthesis of Nanoparticles by Using Plant**

The use of plants or plant extracts, which act as reducing and capping or stabilizing agents for NP synthesis, is more useful over other biosynthesis procedures. This occurs because in this technique,

no need cell culturing and cell maintenance. Moreover, NP synthesis from plants is more stable, allows the production of NPs with different shapes and sizes, and is cheap [43]. The phyto-synthesized nanoparticles, such as Ag, Au, Pt, Cu are widely used in bio-medicine, pharmaceuticals, bio-labelling, food packaging, cosmetics, catalysis and sensory applications [44].

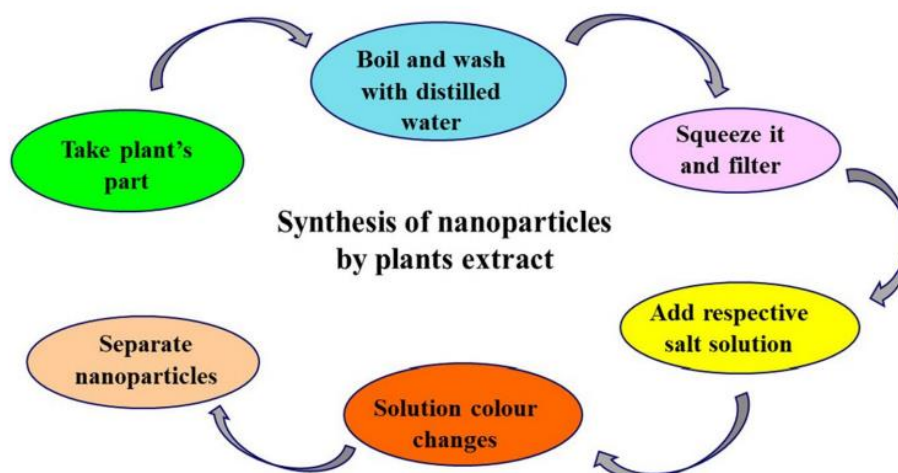


**Figure 2** Environment-friendly and cheap route for the green synthesis of nanoparticles using plants extract.

Metal-doped metal oxide nanoparticles as an extremely interesting type of nanomaterial due to their properties that may exceed the properties of its individual phases by order and they can be applied in a wide variety of fields, including the production of new materials for use in the fields of medicine, energy, and ecology [45]

Silver in its free ionic form is highly toxic to human cells. It has been demonstrated that doping of silver in metal oxide loses the toxicity of free silver to human cells and therefore it is advantageous to use silver doped metal oxide nanoparticles in the antibacterial study. The doping of metal ions into the manganese oxide lattice can be useful, as manganese oxide can be easily prepared, it is environmental friendly, easy to handle and very economical. Also, these doped manganese oxide materials found to show good catalytic activity [46]. Also the NPs made of manganese and silver completely, Ag-MnO combination attracted a significant interest [47]. As an example concerning the positive effects of combining silver and manganese in such a complex, a publication reported

that free silver ions have negative effects on several human cell lines, and by combination with MnO, the silver ions were stabilized, thus reducing their toxicity [48].

### 2.3 Application of Nanomaterials and Nanotechnology

Nanotechnology plays a very important role in modern research; its high ability in many fields, such as pharmacy, electronics, health, food, biomedical sciences, pharmaceuticals, chemistry and chemical industry, energy sciences, cosmetics, environmental health, mechanics and space industry [49].



**Figure 3** Application of nanotechnology in science and environmental science

Among these wide applications, using metal oxide nanoparticles have found considerable results in several applications including nano-chemistry [50]. Potential technological applications of metal oxide nanoparticles play a vital role and attracting researchers with considerable interest from the fields of materials chemistry, medicine, agriculture, information technology, biomedical, optical, electronics, catalysis, environment, energy, and sensor [51]. Consequently, nanosized metal oxide materials are of considerable interest because of significant advantages over bulk analogues and, of course, because they have great prospects for obtaining new types of adsorbents, photo-catalysts, and sensitive layers of gas sensors based on them. However, metal oxides also have a significant drawback. Example fast electron-hole recombination during photo-catalysis [49].

## 2.4 Medicinal Value of *Croton Macrostachyus*

Traditionally *C. macrostachyus* used for treatment of malaria, rabies, gonorrhoea, wound, diarrhoea, hepatitis, jaundice, scabies, toothache, abdominal pain, cancer, typhoid, pneumonia and gastrointestinal disorders and as ethnoveterinary medicine [52]. Pharmacological studies on *C. macrostachyus* indicate that it has a wide range of pharmacological activities such as anthelmintic, antibacterial, antimycobacterial, antidiarrheal, antifungal, anticonvulsant and sedative, antidiabetic, anti-inflammatory, antileishmanial, antioxidant, antiplasmodial, and larvicidal effects [53]. The leaves and shoots of *C. macrostachyus* are used to treat fever and oedema and also mashed leaves used for treatment of hemorrhoids. Moreover, the maceration of *C. macrostachyus* stem bark is used as abortifacient and uterotonic to expel retained placenta. *C. macrostachyus* have the activities of against diarrhoea; traditional healers in Ethiopia use a wide range of medicinal plants with antidiarrheal properties [54]. The chemical constituent in the *C. macrostachyus*, Terpenoids such as abietic acid and steroids like phytosterols have been showed to inhibit production of prostaglandin E2 which have a crucial role in stimulation of intestinal secretion, therefore it has antidiarrheal activities [55].

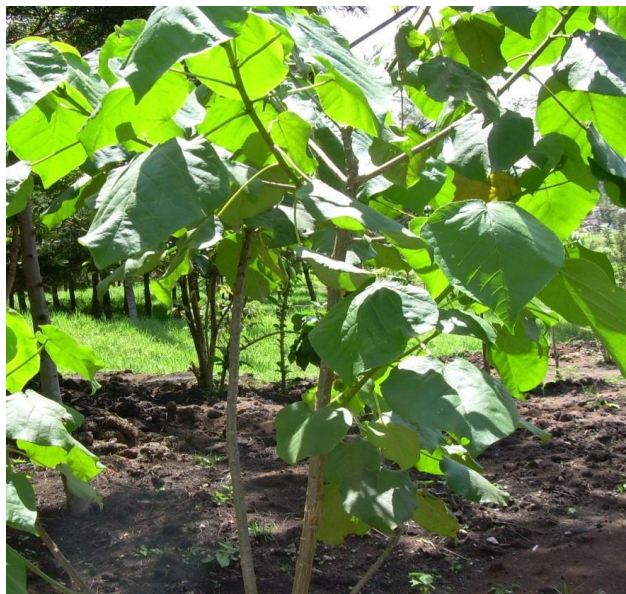


**Figure 4** *Croton macrostachyus* plant.

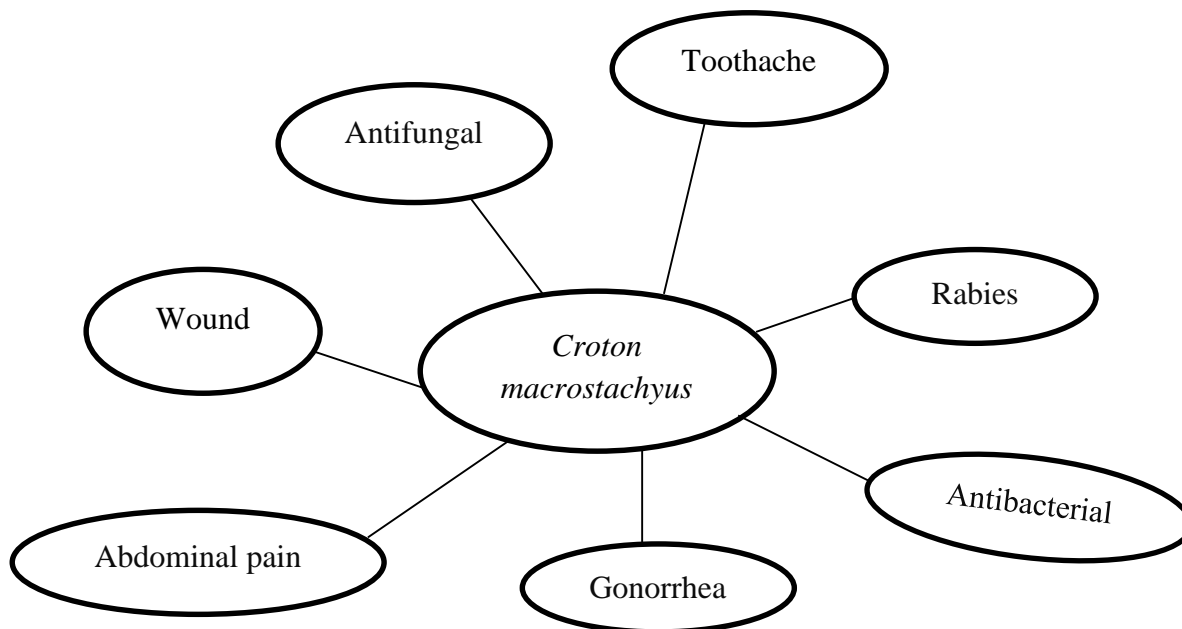


**Figure 5** some use *Croton Macrostachyus* plant.

## 2.5 Characterization Technique for Metal and Metal Oxide Nanoparticles

### 2.5.1 UV-Visible Spectroscopy

UV-Vis spectroscopy is the most convenient technique for the characterization of NPs. The UV-Visible absorption spectra of the samples were measured on a Shimadzu UV-Vis V-530A spectrophotometer. The nanoparticles were dissolved in distilled water sonicated and transfer into cuvette inserted into UV-Visible spectrophotometer. The absorbance was measured at 200- 400 nm [23].

### 2.5.2 Fourier Transformation Infrared (FT-IR) Spectroscopy

Infrared spectroscopy is a crucial tool to characterize the structure of matter at the molecular scale. FTIR spectroscopy analysis is a method based on the principle of infrared spectroscopy, and it has extended its area of application to the study of nano-scaled objects during the last decade [56].

FT-IR spectroscopy is used to identify the possible functional groups of the active components present in the extracts or on the surface of NPs that are responsible for reducing, capping, and



stabilizing being synthesized nanoparticles. The possible functional groups that are present in the plant extract and synthesized nanoparticles were identified in the ranges of 4000-400  $\text{cm}^{-1}$  [57].

### 2.5.3 X-ray diffraction (XRD)

X-ray diffraction is based on constructive interference of monochromatic X-rays and a crystalline sample. These X-rays are generated by a cathode ray tube, filtered to produce monochromatic radiation, collimated to concentrate, and directed toward the sample [58].

X-ray diffraction (XRD) technique is used to realize structural properties of materials and get information like crystal structure/phase, lattice parameters, crystallite size, orientation of single and poly crystals, defects, strains and so on [59]. The crystallite size distribution can be extracted from XRD spectra by analyzing the line profile of the diffraction peak. This was calculated from the most intense peaks using Debye- Scherer's formula below

$$D = \frac{k\lambda}{\beta \cos\theta} \dots\dots\dots(1)$$

Where, D is crystallite size in nanometer, k is shape factor constant, which is 0.89,  $\beta$  is the full width at half maximum (FWHM) in radian,  $\lambda$  is the wavelength of the X-ray and  $\theta$  is the Bragg angle [60].

### 2.5.4 Scanning Electron Microscopy (SEM)

Thin films of the sample were prepared on a carbon coated copper grid by dropping a very small amount of the sample on the grid, extra solution was removed using a blotting paper and then the film on the SEM grid were allowed to dry for analysis [61].

The scanning electron microscope (SEM) is a very useful instrument to get information about topography, morphology and composition information of materials. It is a type of electron microscope capable of producing high-resolution images of a sample surface. Due to how the image is created, SEM images have a characteristic three-dimensional appearance and are useful for judging the surface morphology of the sample [62]. The morphology of synthesized nanoparticles were analyzed by SEM.

## 2.6 Biological assay

The antibacterial activity of the synthesized MnO NPs were tested by disc diffusion method against two gram-positive bacteria (*Staphylococcus aureus* and *Bacillus subtilis*), two gram negative bacteria (*Escherichia coli* and *Staphylococcus bacillus*) and antifungal activity was carried out by agar well diffusion method against four fungi (*Candida albicans*, *Curvularia lunata*, *Aspergillus niger* and *Trichophyton simii*). For disc diffusion method, stock cultures incubated in nutrient agar were transferred to test tube of Muller-Hinton broth (MHB) for bacteria that were incubated for 24 hours at 37°C. The cultures were diluted with fresh Muller-Hinton broth to get  $2.0 \times 10^6$  CFU/ml for bacteria. The Muller Hinton Agar (MHA) plates were prepared by pouring 15 ml of molten media into sterile petri plates. The sample was loaded placed on the surface of the cultured agar plates and incubated at 37 °C for 24 hours then inhibition zones formed around the disc were measured and the results were compared with standard antibiotic, Chloramphenicol. For agar well diffusion method the fungal strains were suspended in sabouraud's dextrose broth for 6 hours to give concentration  $10^5$  CFU/ml and then inoculated with the culture medium. A total of 8 mm diameter wells were punched into the agar and filled with the sample and solvent blanks (hydro alcohol and hexane). Standard antibiotic, Fluconazole (concentration 1 mg/mL) was used as positive control and fungal plates were incubated at 37 °C for 72 hours. The diameters of zone of inhibition observed were measured [63].

### 2.6.1 Antimicrobial resistance

Antimicrobial resistance is one of the most common disastrous factors to global public health. Bacterial resistance to antibiotics has increased rapidly within recent years which have led to the increase in the incidence of infectious diseases caused by those multi-drug resistant bacteria. Infections caused by multi-drug resistant bacteria involve higher morbidity, mortality, and a burden to health care systems. The common cause for antimicrobial resistance effect of bacteria is drug residue, due to contamination of meat products with antibiotic residues when the human consume meat with drug residue, then the appearance of resistant bacteria may occur [64-66].

The main mechanisms of microorganism for antimicrobial resistance are antibiotic inactivation, target modification, changes in permeability and altering metabolic pathway, decreased antibiotic penetration,  $\beta$  lactamase production and efflux pumps [67]. The antimicrobial drug resistance can

be caused by intrinsic and acquired methods. Intrinsic mechanisms are those specified by naturally occurring genes found on the bacterial chromosome. Intrinsic mechanism is due to the presence of outer cell membrane in gram negative bacteria and expression of efflux pumps. The acquired resistance mechanism is due to chromosomal mutation and horizontal transfer of mobile genetic elements from other bacteria in the environment *via* carrying the resistance gene including plasmids, transposon and integrons. The genetic element can be transferred from one bacterium to other through conjugation (cell-to-cell contact between elements), transduction (bacteriophage facilitated transfer of genetic information) and transformation (uptake of free deoxyribonucleic acid (DNA) from the environment [68, 69 and 70]. Gram negative bacteria possesses high permeability barrier for numerous antibiotic molecules. Their periplasmic space contains enzymes which are capable of breaking down foreign molecules, so gram negatives are less susceptible to plant extra.

*Escherichia coli* a gram negative non-spore forming facultative anaerobic rod. Genus *E. coli* belongs to the bacterial group formally called “coliforms” which are member of the “enterics” known as Enterobacteriaceae family [71]. The strain of *E. coli* is motile because they have flagella arranged in peritrichous, but those lack of flagella are non-motile [72]. *E. coli* is a catalase positive, oxidase negative, lactose fermenter, coccobacillus gram negative non spore forming rod shaped bacteria [73]. *E. coli* requires the ability to adapt to variations or extreme changes in temperature, pH and osmolarity conditions commonly encountered nature. For example, the exopolysaccharide (EPS) production of *E. coli* is associated with heat and acid tolerance, and the alteration of lipid composition in membranes is induced by heat stress [74]. *E. coli* can survive for a long time in water, especially at cold temperatures. Water trough sediments contaminated with bovine feces can serve as a long-term (>8-months) reservoir of *E. coli*, and the surviving bacteria in contaminated troughs is a source of infection [75].

In general, all review literature mentioned were supported the present work. The aimed of this study to synthesis MnO NPs and Ag-MnO NCs by using croton macrostachyus leaf extracts.

### **3. MATERIALS AND METHODS**

#### **3.1 Chemicals and Materials**

Potassium permanganate (KMnO<sub>4</sub>, 99%), Ethanol (98%), Dimethylsulfoxide (DMSO), Nutrient agar, Sodium hydroxide (NaOH; 99%, Sigma-Aldrich, India), Potassium iodide (KI), Silver nitrate (AgNO<sub>3</sub>, 99%), Acetic anhydride solution, Ferric chloride (FeCl<sub>3</sub>), Acetone, Ammonia (NH<sub>3</sub>), Hydrochloric acid (HCl), Croton macrostachyus leaf and Distilled water (D. H<sub>2</sub>O). These chemicals were used as analytical reagents.

#### **3.2 Apparatus**

Oven, Mortar and Pestle, Digital balance, Hot Plate and Magnetic stirrer, Watch, Centrifuge, Filter paper, Beakers, Test tubes, Droppers, Graduated cylinders, pH meter, Aluminium foil, label, Rack, crucible, Cuvettes, Refrigerator, Erlenmeyer flask and Desiccator.

#### **3.3 Instruments**

X-ray diffraction (XRD-7000 Cu K $\alpha$  0.9,  $\lambda=0.154$  nm radiations), UV-Vis (Spectrophotometer 6705, JENWAY), FT-IR spectrometers (Carry 630 KBr Engine Malaysia), SEM (Bench Top SEM, JEOL Model: JCM-6000 Plus, Japan) and Cyclic Voltamogram.

#### **3.4 Sample Collection and Preparation**

Fresh leaves of *C. macrostachyus* were collected from Ilu Aba Bor Zone, around Mettu town away from Jimma 260 Km and 600 Km from Addis Ababa Ethiopia. The collected fresh leaves were thoroughly washed by tap water followed distilled water to remove any dirt particles. The washed leaves were air dried and stored in polyethylene bag.

The dried *C. macrostachyus* leaf was crushed using pestle and mortar and stored in polyethylene bags until used. The 10 g dry *C. macrostachyus* leaf was weighed using electronic balance and transferred to 250 mL beaker; 200 mL of distilled water was added into the beaker. The mixture was heated for 15 minutes with stirring using a magnetic stirrer at 60 °C and the extract was chilled for 30 minutes at room temperature. Then, the clear extract were collected by filtration using Whatman no. 1 filter paper and then stored in the refrigerator at 4 °C for further uses.

### **3.5 Preliminary Phytochemical Screening**

The qualitative phytochemical investigation of aqueous solution extract of *Croton macrostachyus* leaves were carried out.

#### **3.5.1 Test for Phenols**

5 mL *C. macrostachyus* leaf extract was added to test tube and a few drops of 0.1 % ferric chloride were added. The blue-black precipitate was formed which indicated the presence of phenols [76].

#### **3.5.2 Test for Flavonoids**

2 mL of ethyl acetate was added to 5 mL of *C. macrostachyus* leaf extract and 1 mL of dilute ammonia solution was added drop by drop. The mixture was shaken and the layers were formed separate and the yellow color in the ammonia layer indicated the presence of flavonoids [77].

#### **3.5.3 Test for Alkaloids**

4 mL *C. macrostachyus* leaf extract and 2 mL of acetic anhydride solution were added to test tube. The reddish brown precipitate was regarded as positive for the presence of alkaloids [78].

### **3.6 Parameters Optimization for the synthesis of MnO NPs**

#### **3.6.1 pH optimization**

The influence of pH for the synthesis of Mn ONPs were studied in range of pH from 8 to 10. The pH was adjusted by adding 0.1 M NaOH solution and pH 9 optimum, because it shows maximum peak and was good for the synthesis of MnO NPs [79].

#### **3.6.2 Plant Extract Volume**

Synthesis of MnO NPs was mediated by the use of different volume of *C. macrostachyus* leaf extract. Different volume 10 mL, 15 mL and 20 mL of freshly prepared. Among 10 mL, 15 mL, and 20 mL volumes used, 20 mL of the extract was found to good for the synthesis of MnO NPs [80].

### 3.6.3 Concentration of Precursor

The ratio of precursor concentrations should correspond to the amount of plant extract used [40]. In this study, 40 mL of different precursor concentrations (0.005, 0.01, and 0.02) M were reacted with 20 mL of leaf extract and 0.01 M was optimized because it gave a sharp peak which shows the formation of nanoparticles since the intensity of the surface Plasmon peak has direct proportionality with the concentrations of synthesized nanoparticles in the solution.

### 3.7 Synthesis MnO NPs

Aqueous solutions of 0.01 M potassium permanganate were prepared from 0.39 g of  $\text{KMnO}_4$  in 250 mL volumetric flask by using distilled water to synthesize manganese oxide nanoparticles. 40 mL of precursor solution and 20 mL of *C. Macrostachyus* extract were mixed in a beaker. The mixtures were heated with magnetic stirrer at 60 °C for 1 hour and chilled at room temperature for 30 minutes. The precipitate was centrifuged at 3000 rpm for 15 minutes and washed with distilled water 3 times followed by ethanol to obtain pure MnO NPs [81]. The paste was transferred into crucible and dried in oven at 80 °C for 1 hour. The product was crushed into fine powder and kept in a desiccator for further characterization and application.

#### 3.7.1 Synthesis of Ag-MnO Nanocomposite

Synthesis of Ag-MnO NCs using *Croton Macrostachyus* leaf extract was carried out based on the literature with slight modifications [24]. 0.01 M of potassium permanganate ( $\text{KMnO}_4$ ) solution was prepared in 40 mL of distilled water. After its complete dissolution, 0.01 M of silver nitrate ( $\text{AgNO}_3$ ) prepared from 40 mL of distilled water were added together. Then, 20 mL of *Croton Macrostachyus* plant extract was mixed into the mixture of the solution and the reaction mixture was heated with stirring using magnetic stirrer at 60 °C for 1 hour and the color of the mixture changed to brown, which indicates the formation of Ag-MnO NCs. The precipitate was centrifuged at 3000 rpm for 15 minutes and washed with distilled water 3 times followed by ethanol to obtain pure Ag-MnO NCs and dried in oven at 80 °C for 1 hour. Finally, it was ground in a mortar and pestle to give the final nanocomposite, which was used for different characterizations.

### 3.8 Characterization Technique for Metal and Metal Oxide Nanoparticles

#### 3.8.1 UV-Vis Spectroscopy Studies

UV-Vis spectroscopic is the most convenient technique for the characterization of NPs. The UV-Vis absorption spectra of the samples were measured on a Spectrophotometer 6705, JENWAY spectrophotometer. The MnO NPs and Ag-MnO NCs were dissolved in distilled water sonicated and transfer into cuvette inserted into UV-Visible spectrophotometer. The absorbance was measured at 200- 400 nm [23].

#### 3.8.2 Fourier Transform Infrared (FT-IR) Spectroscopy Studies

Fourier transform infrared (FT-IR) spectra of the samples were recorded with a Carry 630 KBr Engine Malaysia FT-IR spectrometer in the range of 4000 – 400  $\text{cm}^{-1}$ . The purified dried powder of MnO NPs and Ag-MnO NCs were used for characterizations of the functional group [57].

#### 3.8.3 X-ray diffraction (XRD) Studies

X-ray diffraction (XRD) technique is used to realize structural properties of materials and get information like crystal structure/phase, lattice parameters, crystallite size, orientation of single and poly crystals, defects, strains and so on [60]. The crystallite size distribution can be extracted from XRD spectra by analyzing the line profile of the diffraction peak. This was calculated from the most intense peaks using Debye- Scherer's formula below.

$$D = \frac{k\lambda}{\beta \cos\theta} \text{-----} (1)$$

Where, D is crystallite size in nanoparticle, K is Scherer constant with value from 0.9-1,  $\beta$  is the full width at half maximum (FWHM) in radian,  $\lambda$  is the wavelength of X-ray source (0.154 nm) and  $\theta$  is the Bragg angle.

#### 3.8.4 Scanning Electron Microscopy (SEM) Studies

The scanning electron microscope (SEM) is a very useful instrument to get information about topography, morphology and composition information of materials. It is a type of electron microscope capable of producing high-resolution images of a sample surface. Due to how the

image is created, SEM images have a characteristic three-dimensional appearance and are useful for judging the surface morphology of the sample [62]. The morphology of synthesized MnO NPs and Ag-MnO NCs were analyzed by SEM.

### **3.9 Electrochemical Studies of MnO NPs**

The surface of a clean gold electrode was polished with an alumina slurry. After the polished gold electrode was sonicated with DW and dried, 0.5 g of powdered MnO NPs was dissolved in 1 mL of distilled water to create a slurry. The gold electrode was modified with MnO NPs slurry. MnO NPs was applied to the electrode surface so that the MnO NP slurry covered the entire electrode surface and measure the oxidation and reduction of synthesized nanoparticles. Ag/AgCl containing saturated KCl was used as a reference electrode. A Pt wire was used for the counter electrode, and MnO NPs / gold electrode was used for the working electrode. A pH 7 0.1M phosphate buffer was used for the measurement [83].

### **3.10 Antimicrobial activity**

The antibacterial activity of the samples was evaluated by disc diffusion method of against two gram-positive bacteria (*S. aureus* and *B. cereus*) and two gram-negative bacteria (*E. coli* and *S. typhi*). The bacterial cultures were prepared by diluting with autoclaved fresh Muller-Hinton broth medium and the prepared bacterial cultures were inoculated with synthesized MnO NPs and Ag-MnO NCs and standard antibiotic on Muller-Hinton agar plates. 1 mL/mg concentration of plant leaf extract, synthesized MnO NPs and Ag-MnO NCs of 200 mg/mL were loaded on 6 mm sterile disc and placed on the surface of the medium to get diffusion. The plates were kept for incubation at 37 °C for 24 hours. After incubation, the plates were studied for the presence of a zone of inhibition. 200 mg/mL concentration of Gentamicin and 1 mL DMSO were used as standard antibiotics for two gram positive and gram negative bacterial respectively [63].

The antifungal activity was carried out by agar well diffusion method for *C. albicans*, The sample of plant leaf extract, synthesized MnO NPs and Ag-MnO NCs of 200 mg/mL were loaded on 6 mm sterile disc were incubated at 37 °C for 72 hours. Standard antibiotic Clotrimazole concentration 200 mg/mL was used as antifungal control. The diameters of zone of inhibition observed were measured and studied [74].



### **3.11 Preparations of Test Solution**

Five test solutions were prepared for bacterial and fungal testing. Prepared sample of 500  $\mu$ L plant leaf extract concentration in 1 mL DMSO and 4 solutions with concentrations of 200 mg/L MnO NP, 1% Ag, 2% Ag and 3% Ag spiked from 5 solutions. Inhibition zones were measured after 24 hours of incubation. Bacterial and fungal activity was determined from the inhibition zones measured on the disc. A clear zone of inhibition formed around each disc was measured in mm.

## 4. RESULTS AND DISCUSSION

### 4.1 Phytochemical Analysis of *Croton Macrostachyus* Leaves Extract

The phytochemical tests were performed to identify classes of secondary metabolites present in the leaves of *Croton Macrostachyus* plant extract. Phytochemical screening of the extract showed the existence of phenols, flavonoids and alkaloids (**Appendix 3**). A) Phenol test B) flavonoids test C) alkaloids test. This may indicate that the plant extract contains the phytochemicals which is promising as stabilizing and capping agent for NPs and NCs formation.

**Table 1** Phytochemical components of *Croton Macrostachyus* plant extract

Phytochemicals	Reagents and chemicals used	Results
Phenols	FeCl <sub>3</sub> (0.1%) solution	+
Flavonoids	Dilute NH <sub>3</sub> solution, ethyl acetate	+
Alkaloids	Acetic anhydride solution	+

**Note:** (+) indicates presence of Phytochemicals

### 4.2 Synthesis Manganese Oxide Nanoparticles

The color of the mixture of leaf extract and potassium permanganate (KMnO<sub>4</sub>) was initially purple. After heating at 60 ° C for 1 hour with continuous stirring, a dark brown color was observed, indicating the formation of MnO NPs. The phytochemicals present in the plant extract function can used as a reducing agent that converts metal ions into the corresponding nanoparticles, as well as an effective capping agent that prevents NPs agglomerations [22].

### 4.3 Optimization of parameters during synthesis of MnO NPs

In this study, the major parameters such as pH, Precursors concentrations, volume of plant extract, were optimized as follows to get optimum product of MnO NPs with small particle size.

### 4.3.1 Effect of pH

The pH is one of the factors that influence the size, shape, and composition of a nanoparticle. pH in aqueous media can highly influence the progress of the metal ion reduction reaction [79]. The role of pH on nanoparticles synthesis could be seen in its effect on the capping and stabilizing abilities, and subsequently the growth of the nanoparticles. The presence of OH<sup>-</sup> ion in an alkaline pH environment might enhance the reducing and stabilizing capabilities of the biomolecules in the leaf extract [84]. Synthesis of MnO NPs using aqueous extract of *Croton macrostachyus* leaves was examined over a pH range from 8 to 10. As the pH was increased from pH 8 to pH 10, a blueshift (from 228 nm to 230 nm) was observed on the peak. This blueshift mostly enhances the nanoparticle size; since a highly broad spectrum was formed at especially pH 8. By increasing to pH 9 blueshift was observed at  $\lambda_{\max}$  230 nm that could be attributed to the decrease in the particle size. Therefore, pH 9 was taken as optimum condition to bio-synthesize MnO NPs. The result obtained was in a match with the findings reported in the literature [85], that MnO NPs was synthesized at optimum pH of 9. Therefore, the result obtained show that alkaline pH, great numbers of nuclei formed, instead of aggregation [84].

**Table 2** Optimization of pH

Molarity of KMnO <sub>4</sub>	Leaf extract	pH	UV – Visible	Absorbance
0.01 M	20 mL	8	229 nm	0.7128
0.01 M	20 mL	9	230 nm	0.8387
0.01 M	20 mL	10	228 nm	0.7969

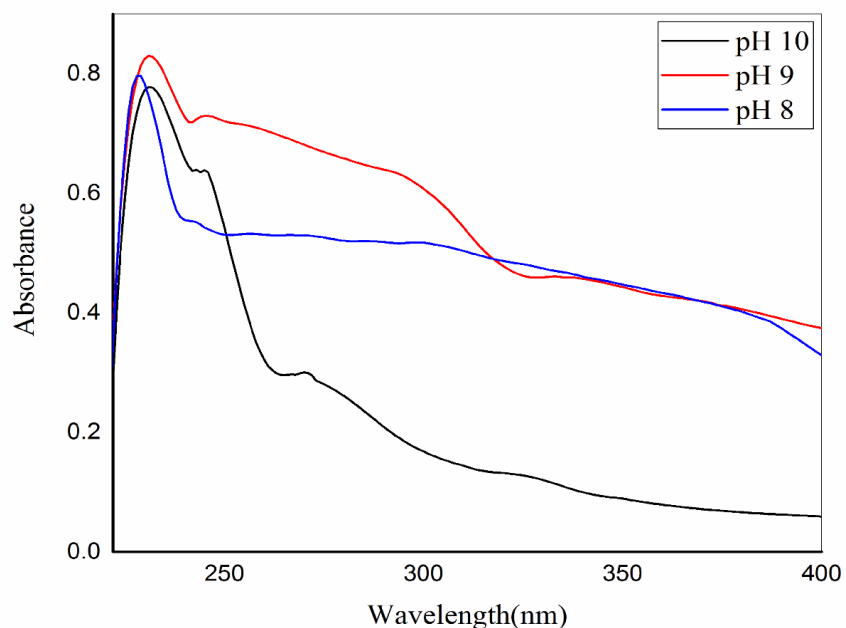


**Figure 6** UV-Visible spectra of the optimization pH of Manganese Oxide Nanoparticles.

#### 4.3.2 Plant Extract Volume

The synthesis of NPs using plant extracts is primarily influenced by the type and amount of biomolecules present in the plant extracts. The amount of plant extract used in the synthesis of nanoparticles plays an important role in reducing the oxidation number of metal ions [80]. Effect of the volume of *Croton macrostachyus* extract were studied by varying the volume from 10, 15, 20 mL and other factors kept constant and its effect was identified by UV-Vis spectroscopy [85]. Various amounts (10, 15, and 20) mL were reacted with 40 mL of precursor solution to determine the optimal amount of leaf extract and 20 mL is optimized.

**Table 3** The optimization of plant extract volume

Molarity of $\text{KMnO}_4$	Leaf extract	pH	UV- Visible	Absorbance
0.01 M	20 mL	9	231 nm	0.8134
0.01 M	10 mL	9	232 nm	0.7469
0.01 M	15 mL	9	233 nm	0.7857

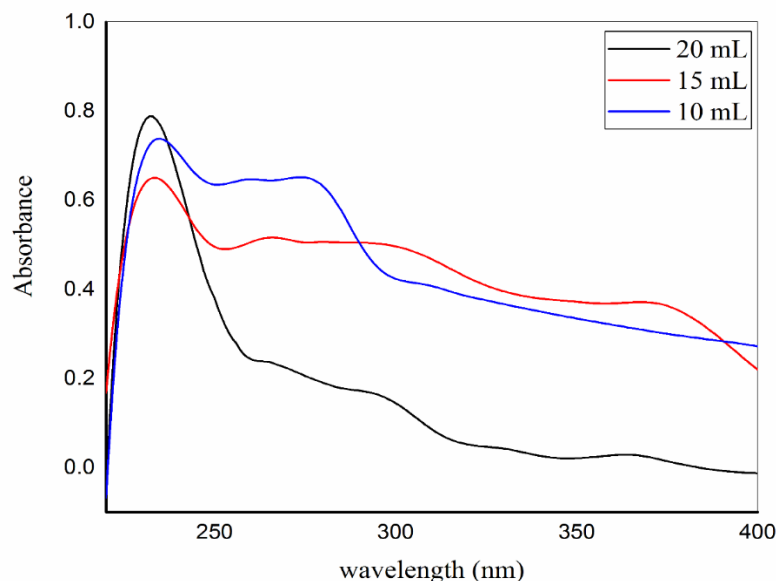


**Figure 7** UV-Vis of MnO NPs of the optimization of plant extract volume.

#### 4.3.3 Concentration of $\text{KMnO}_4$ Optimization

40 mL of solution of different precursor concentrations (0.005, 0.01 and 0.02) M was reacted with 20 mL leaf extracts respectively and 0.01 M was taken as optimum concentration because it gave a sharp peak which shows the formation of MnO NPs, since the intensity of the surface Plasmon peak has direct proportionality with the concentrations of synthesized nanoparticles in the solution [85]. The result obtained was in close agreement with a recent report [80]. Because the intensity of the UV-Vis peak increased, this shows the formation of small-sized nanoparticles and increase in intensity suggests that more nanoparticles are formed.

**Table 4** The  $\text{KMnO}_4$  (precursor) concentration optimization

Molarity of $\text{KMnO}_4$	Leaf extract	pH	UV – Visible	Absorbance
0.005 M	20 mL	9	229 nm	0.7262
0.01 M	20 mL	9	230 nm	0.7761
0.02 M	20 mL	9	233 nm	0.7353

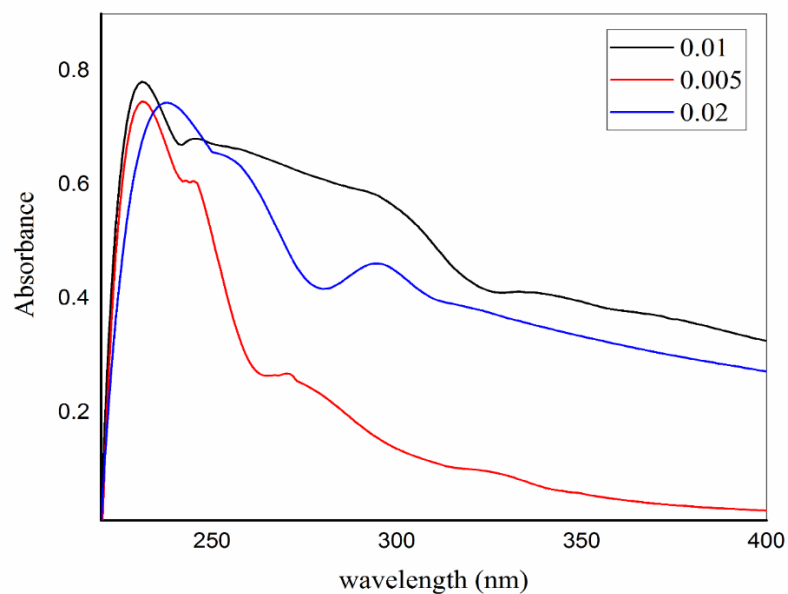


**Figure 8** UV – Vis spectra of MnO NPs the optimization of precursor concentration.

#### 4.4 UV–Visible Spectroscopy Analysis

The spectra of UV-Visible absorption of the synthesized MnO NPs had been measured on (UV-Vis, Spectrophotometer 6705 JENWAY) spectrophotometer is range from 200 – 400 nm. The synthesized nanoparticles had been exhibited peaks at 230 nm which had been exhibited humps in (Fig. 6). There broad peaks, however the peaks at 230 nm had greater absorbance and indicated the formation of MnO nanoparticles. Similar results were obtained for chamomile flower extracts mediated synthesis of MnO nanoparticles [82].

#### 4.5 FT-IR Analysis of Synthesized MnO NPs from *Croton Macrostachyus*

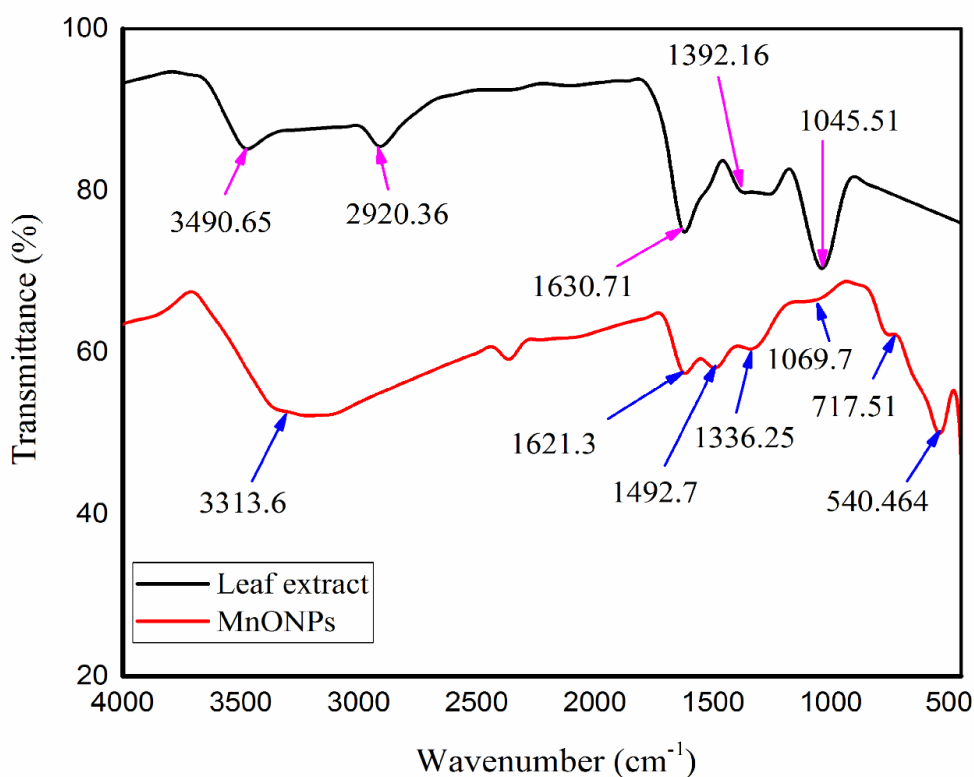


**Figure 9** FT-IR spectra of MnO NPs synthesized from *C. macrostachyus* leaf extract

Fourier Transform Infrared (FT-IR) spectroscopy is known for its high sensitivity, especially in detecting inorganic and organic species with low content. The FT-IR spectra of *C. macrostachyus* stabilized MnO NPs is represented in (**Fig. 9**). The spectrum was recorded in the range of 4000 – 400  $\text{cm}^{-1}$ . The peaks observed at 540, 717, 1069, 1336, 1492, 1621 and 3313  $\text{cm}^{-1}$ . From the data obtained, the peak observed at 3313  $\text{cm}^{-1}$  which can be assigned to the -OH stretching of water or ethanol present in the system. The C = O of *C. macrostachyus* at 1630  $\text{cm}^{-1}$  shifted to wavenumbers at 1621  $\text{cm}^{-1}$  due to the interaction with Mn-O. The absorption peak at 1336  $\text{cm}^{-1}$  represents the bending band of water adsorbed by MnO NPs. The presence of the (C-O) band belonging to *C. macrostachyus* was assigned by the peaks found at 1045  $\text{cm}^{-1}$  and 1069  $\text{cm}^{-1}$ . The two important absorption peaks observed at 717  $\text{cm}^{-1}$  and 540  $\text{cm}^{-1}$  correspond to the characteristic stretch bonds of Mn-O, indicating the presence of MnO nanoparticles in the sample. The spectra of Mn-O is in good agreement with results reported by other researchers [63, 23 & 87].

#### 4.6 XRD Analysis of Synthesized MnO NPs from *C. Macrostachyus*

The crystal structure of manganese oxide nanoparticles synthesized from *C. macrostachyus* leaf extract was investigated by X-ray diffraction measurement using an X-ray diffractometer (machine model XRD-7000). XRD spectra were recorded in the range of 10 ° to 80 ° at an angle of 2 $\theta$  using CuK $\alpha$  ( $\lambda = 1.54 \text{ \AA}$  or 0.154 nm) and the scan rate of 0.04 0 / min. X-ray analysis of the synthesized MnO nanoparticles showed diffraction peaks at 37.48 °, 44.04 °, 66.96° and 77.72°, corresponding to amorphous crystalline. The XRD pattern show the amorphous nature of representative samples. The XRD pattern of MnO NPs (**Fig. 10**) illustrates well-defined characteristic diffraction planes indexed to the (100), (101), (110) of face-centered cubic MnO matched with the JCPDS File No. 030-0820. The XRD patterns displayed in this study agreed with the earlier research reported [24]. Using *Brassica oleracea* leaf extract, amorphous manganese oxide was obtained by a biogenic process also supports this study [88].

**Table 5** Comparison of size of MnO NP with different works

Plant used	Crystalline nature	Reference
<i>Brassica oleracea</i>	Amorphous	[84]
<i>Cucurbita pepo</i>	Amorphous	[24]
<i>Croton macrostachyus</i>	Amorphous	This work



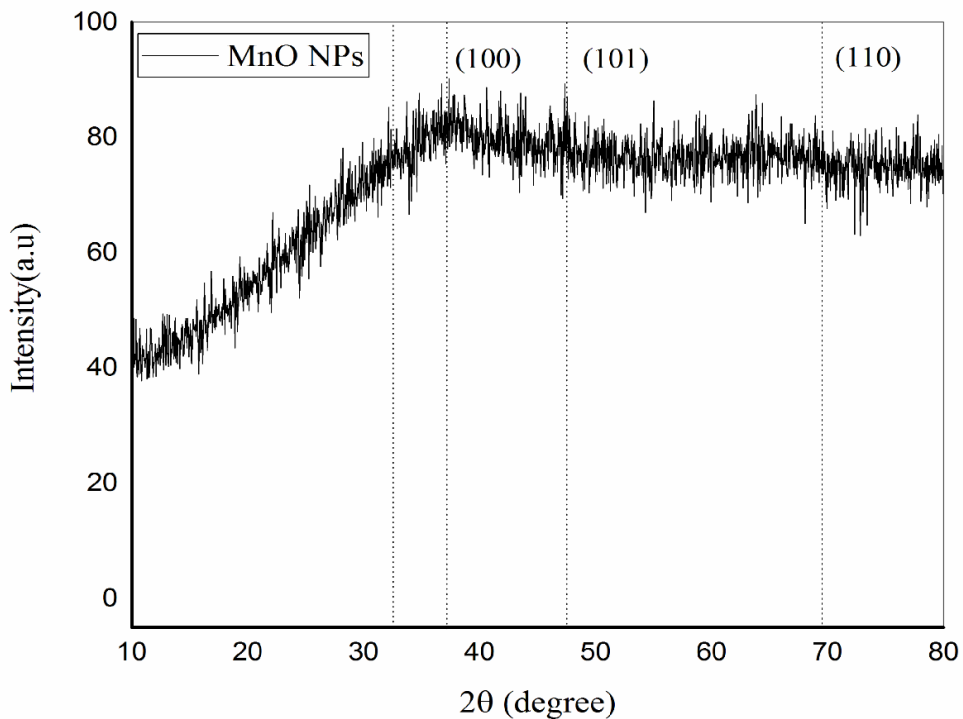


**Figure 10** XRD pattern of synthesized undoped MnO NPs

#### 4.7 Synthesis of Ag-Doped MnO Nanocomposite

The color of the mixture of leaf extract and  $\text{KMnO}_4$  and  $\text{AgNO}_3$  solutions was initially reddish brown. After heating at  $60\text{ }^\circ\text{C}$  for 1 hour with continuous stirring, brown color was observed, indicating the formation of Ag-MnO NCs. The phytochemicals present in the plant extract function as a reducing agent that converts metal ions into the corresponding nanoparticles, as well as an effective capping agent that prevents NP aggregations.

##### 4.7.1 UV-Vis Analysis of Synthesized Ag-MnO NCs from *C. Macrostachyus*

The formation of Ag-MnO NCs had been shown with the aid of using UV-Visible analysis. The spectra of UV-Visible absorption of the synthesized Ag-MnO NCs had been measured spectrophotometer within the range of 200 – 400 nm. The synthesized nanocomposites had been exhibited peaks at 232 nm and 0.8364 absorbance which had been exhibited humps in (**Fig. 10**).

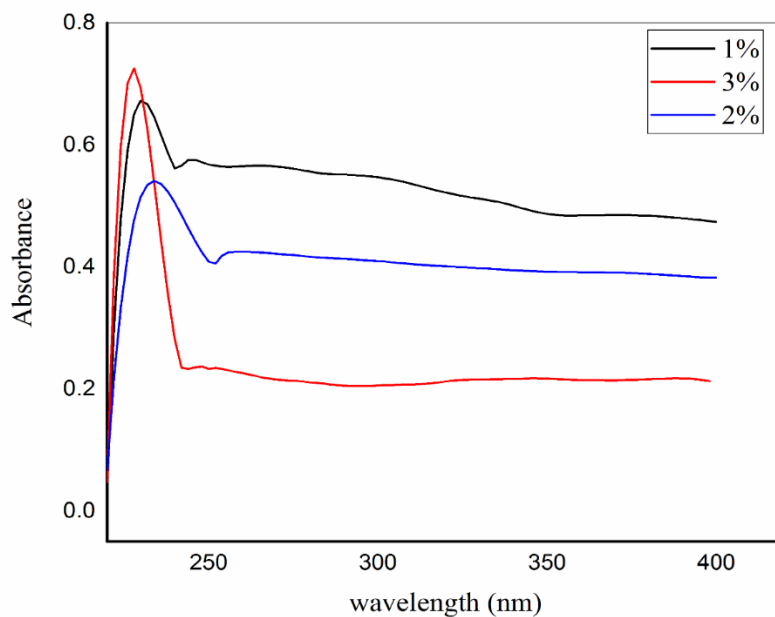


**Figure 11** UV-Visible spectrum of Ag-MnO NCs synthesized from *C. macrostachyus* leaf extract.

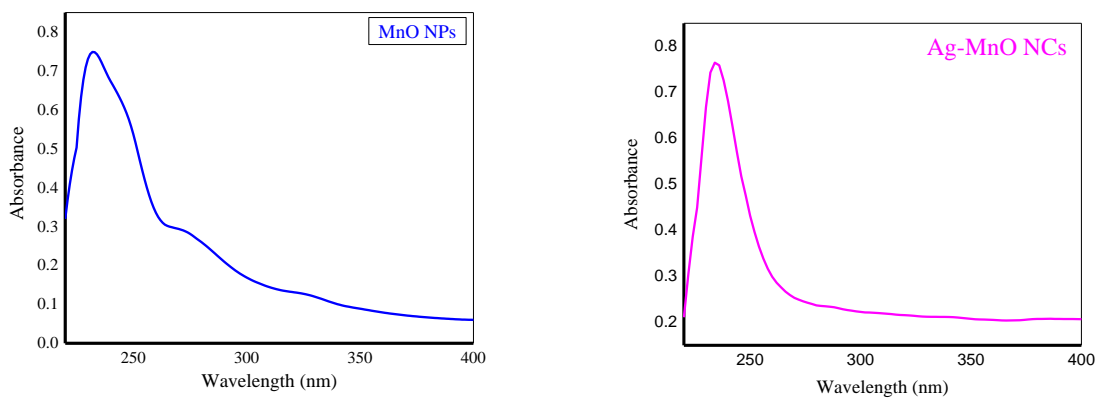


**Figure 12** UV- Vis spectra of A) MnO NPs and Ag-MnO NPs.

The UV-Vis absorption spectra of MnO nanoparticle was broad compared to Ag-MnO NCs peak; this broadness of the absorption peak is because of wide size distribution of these nanoparticles.

#### 4.7.2 FT-IR Analysis of Synthesized Ag-MnO NCs from *C. Macrostachyus*

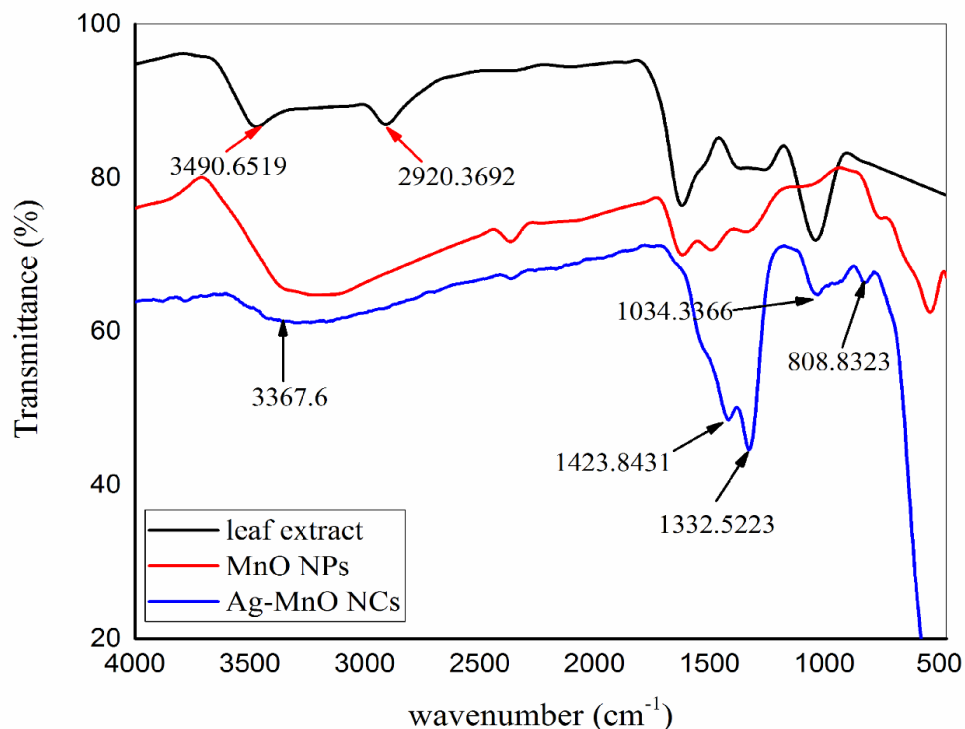


**Figure13** FT-IR spectra of synthesized MnO NPs & Ag-MnO NCs using *C. macrostachyus* leaf extract.

The peaks were observed at 3367, 1423, 1332, 1034 and 808 cm<sup>-1</sup>. The FT-IR spectrum of the synthesized Ag-MnO NCs (**Fig. 13**) showed broad band absorption at 3367 cm<sup>-1</sup> due to the O-H bond stretching vibration. Peaks near 1423 cm<sup>-1</sup> corresponded to the bending mode of phenol-OH or symmetric stretch COOH functional groups. The band observed at 1332 and 1034 cm<sup>-1</sup> which gave stronger absorption showing stabilization of C=O and -C=C functional groups of the biomolecules. The FT-IR of these peaks indicated the presence of organic molecules from the *Croton macrostachyus* leaf extract. In the Ag-MnO NCs sample, peak absorption at 808 cm<sup>-1</sup> was assigned to the vibrational frequency due to the change in the microstructural feature by addition of Ag into MnO lattice. This is related to the previously reported [24].

The peak observed at 1069 and 1034 cm<sup>-1</sup> are ascribed to stretching vibration of C=O bond from biomolecules of plant extract. The low intensity band observed around 1492 and 1336 cm<sup>-1</sup>

occurred in MnO NPs which is shifted to  $1332\text{ cm}^{-1}$  after doping by silver may be due to O-H bending vibrations.

#### 4.7.3 XRD Analysis of Synthesized Ag-MnO NCs from *C. Macrostachyus*

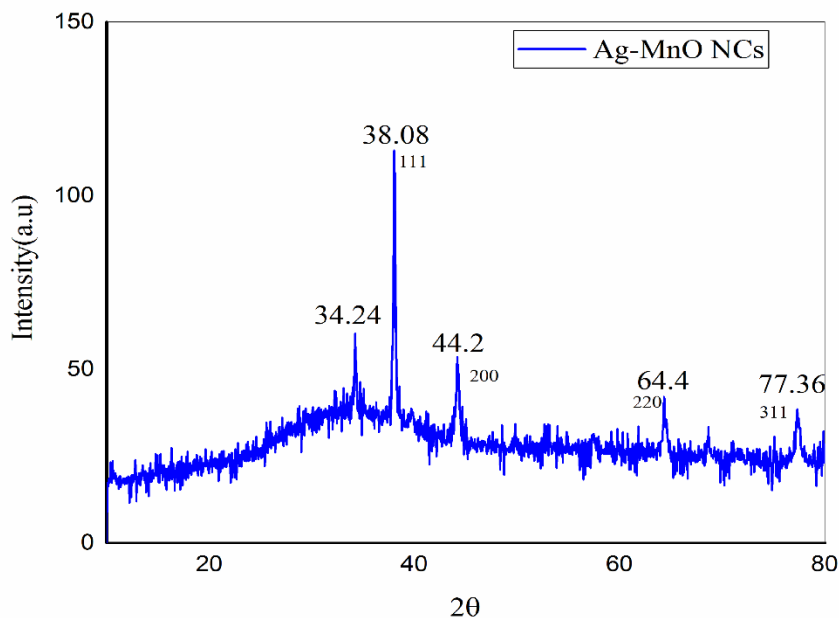


**Figure 14** XRD pattern obtained for *C. macrostachyus* synthesized Ag-MnO NCs

X-ray diffraction studies were performed on the prepared Ag-MnO NCs. The crystalline of NCs has been confirmed by powder X-ray diffraction studies and a diffraction peak has been shown (**Fig. 14**). After Ag-doped MnO NPs, four additional peaks were observed in the Ag-MnO NCs, XRD spectra at  $2\theta = 34.24^\circ$ ,  $38.08^\circ$ ,  $44.2^\circ$ ,  $64.4^\circ$ , and  $77.36^\circ$ . The planes of (111), (200), (220), (311) characteristic of silver face-centered cubic structure. The result obtained was in close agreement with a recent report [85]. The crystallite size distribution obtained from XRD spectra by analyzing the line profile of the diffraction peak. This was calculated from the most intense peaks using Debye- Scherer’s formula below.

$$D = \frac{k\lambda}{\beta \cos\theta} \text{-----(1)}$$

Where, D is crystallite size in nanoparticle, K is Scherer constant with value from 0.94,  $\beta$  is the full width at half maximum (FWHM) in radian,  $\lambda$  is the wavelength of X-ray source (0.154 nm) and  $\theta$  is the Bragg angle.

The crystallite size of Ag-MnO NCs prepared by using *C. macrostachyus* leaf extract leaves was 25.54 nm. This is closely related to the previously reported [90].

#### 4.8 Scanning Electron Microscopy (SEM) Analysis

The surface morphological features of the synthesized MnO NP and Ag-MnO NC samples were examined with a scanning electron microscope. The image was taken at x30000 magnification. SEM images of MnO NPs and Ag-MnO NCs are shown in (Fig 15 a & b). Here, agglomeration occurred during the synthesis process. This indicates that the formed manganese oxide nanoparticles are moderately dispersed and less agglomerated. SEM images of the formed compounds showed that the particles were polymorphic forms of the material. The SEM image shows the morphological sizes of MnO NPs and Ag-MnO NCs. SEM shows that MnO NP is pentagonal and Ag-MnO NC is a mixture of spherical and rod shapes. The morphology structure of the prepared samples shows that the particles are less agglomerated, and nanoparticle size is not regular [78, 91].

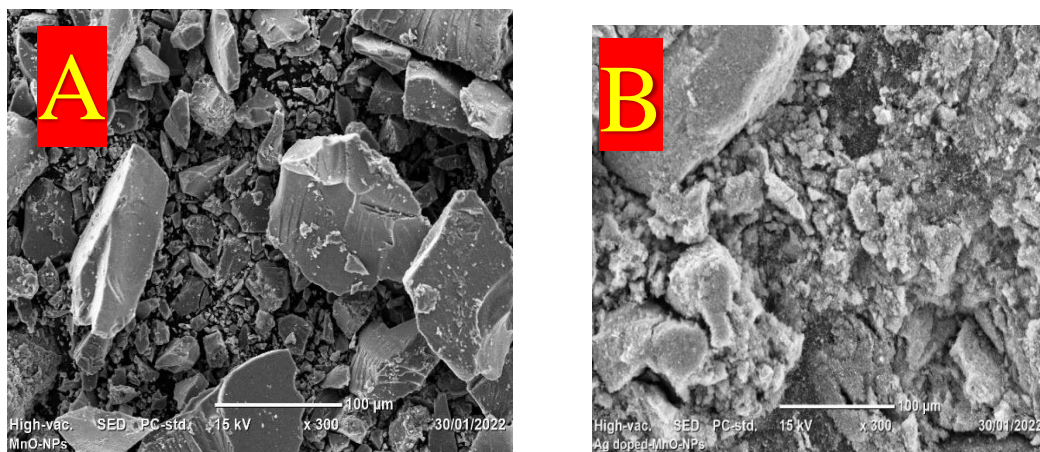


**Figure 15** SEM image of MnO NPs and Ag-MnO NCs synthesized from *C. macrostachyus* leaf extract

#### 4.9 Electrochemical Analysis of Synthesized MnO NPs

Cyclic Voltammetry measurements were conducted at 100 mV s<sup>-1</sup> scan rate. Sensitivity and detection limit of MnO NPs/gold electrode were carried out using DVP technique. 250 mL phosphate solution was tested over -0.2 to 1.6 voltage. However, the addition of phosphate buffer show the electrochemical in (Fig.16). Reduction peak was observed at 0.318 V reversible and

oxidation peak was observed at 0.891 V irreversible. The analysis of scan rate explained that the current increases with increasing scan rate in both oxidation and reduction process. The result agreement with previous reports [83].

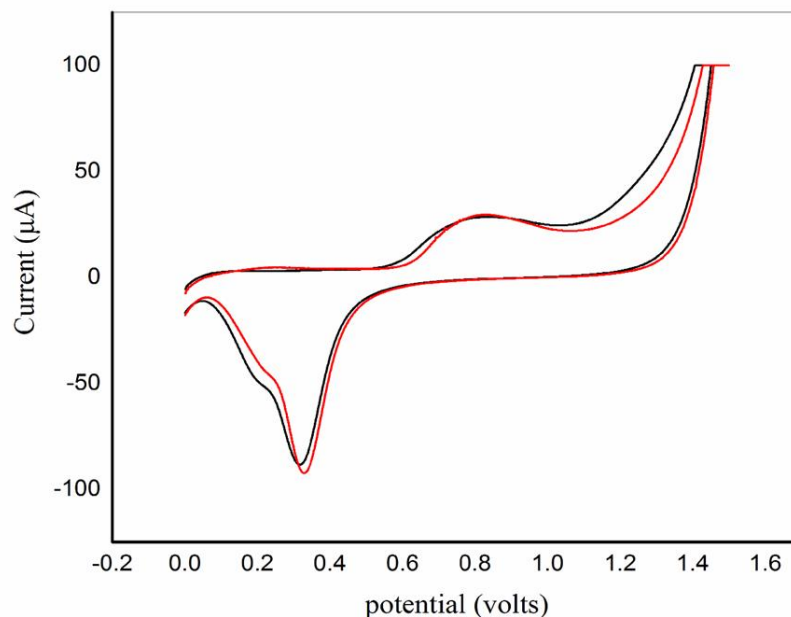


**Figure 16** Cyclic Voltammetry analysis of MnO NPs /gold electrode of oxidized and reduced on phosphate buffer solution.

#### 4.10 Antimicrobial Activity Analysis

The antimicrobial activity of the plant extract and synthesized NPs was determined by measuring the zone of inhibition. No antimicrobial activity was observed for the plant extract and MnO NPs. (Table 6) shows the zones of inhibition of Ag-MnO NCs synthesized using the plant extract, the positive control and *Clotrimazole*. An increase in the concentration of the Ag-MnO NCs resulted in an increase in antimicrobial activity, which was consistent with previous studies [63]. The antibacterial and fungal activity of *C. macrostachyus* leaf extract, MnO NPs and Ag-MnO NCs by using 200 mg/mL were tested. The antibacterial and fungal activities of synthesized MnO NPs and Ag-MnO NCs were performed by disc diffusion method. The clear zone of inhibition was recorded for Ag-MnO NCs. But, plant extract and MnO NPs did not show clear zone of inhibition against two gram positive (*S. aureus* and *B.cereus*) and two gram negative (*E. coli* and *S. typhi*) bacterial

as well as candida albicans test. Previous studies have reported that MnO nanoparticles synthesized from plant extracts exhibit significant antibacterial and fungal activity, supporting current research results [24, 92]. The synthesized Ag-MnO NCs show greater antibacterial and fungal activity than MnO NPs and leaf extract.

**Table 6** Synthesized MnO NPs and Ag-MnO NCs from *C. macrostachyus* leaf extract and their antibacterial and fungal activity.

Organisms	Zone of inhibition in (mm diameter)							
	Positive control		Negative control	Leaf extract	MnO NPs	1% Ag	2% Ag	3% Ag
	Gentamicin	Clotrimazole	DMSO					
<i>S. aureus</i>	26		-	-	-	10	12	13
<i>B.cereus</i>	23		-	-	-	9	10	12
<i>E. coli</i>	24		-	-	-	8	10	11
<i>S. typhi</i>	25		-	-	-	8	10	12
<i>C. albicans</i>		24	-	-	-	10	12	14

**Note:** - indicates no inhibition zone

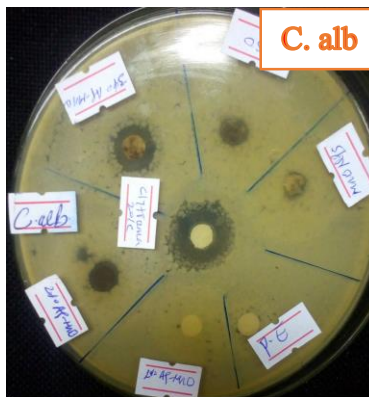
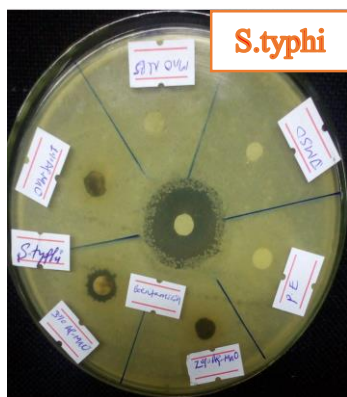
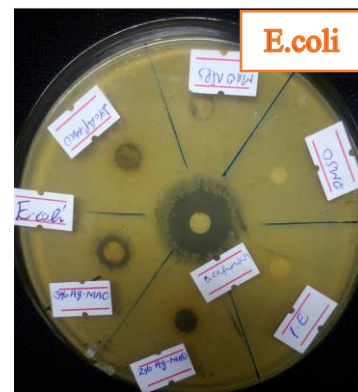
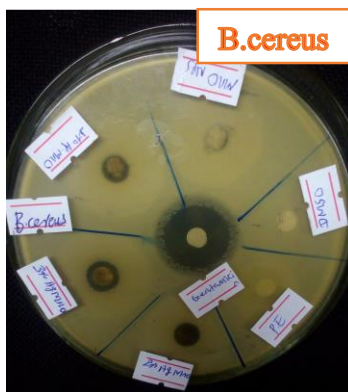
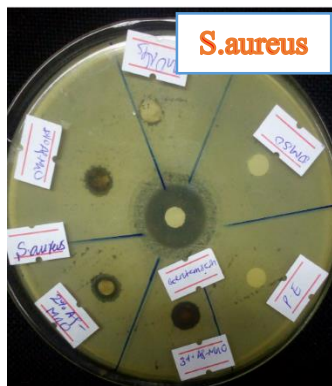


**Figure 17** The antimicrobial test of leaf extract, MnO NPs and Ag-MnO NCs.



## 5. CONCLUSION AND RECOMMENDATIONS

### 5.1 Conclusion

MnO NPs and Ag-MnO NCs were synthesized from potassium permanganate and silver nitrate using *C. macrostachyus* leaf extract can acting as a capping and reducing agent. The Synthesis of MnO nanoparticles were optimized by pH, plant extract volume and precursor concentration (KMnO<sub>4</sub>). The FT-IR spectroscopy revealed the presence of secondary metabolites like phenols, flavonoids, alkaloids, and others were in the synthesized nanoparticles. The XRD result shows the synthesized nanoparticles have amorphous crystalline and Ag-doped shows crystalline. SEM shows MnO NPs has a pentagon shape and Ag-MnO NCs has a mixture of spherical and rod like shape. The reduced and oxidized of MnO NPs was characterized by CV. The synthesized Ag-MnO NCs have been exhibited significant antibacterial activity against all four bacterial strains and one fungal. These are the gram positives bacterial *S. aureus* and *B. cereus*, the gram negatives bacterial *E. coli* and *S. typhi* and *candida albicans*. The synthesized nanocomposite show greater antibacterial and fungal activity. Croton macrostachyus leaf extract and the synthesized MnO NPs have no antibacterial and fungal activities.

## 5.2 Recommendations

For further work, it is encouraged that extra characterization is needed for size determination and composition of the pattern the usage of devices like FESEM, TEM and EDX. Additional work is also required on a few different metal-doped, metal oxide nanoparticles through the mediation of *Croton macrostachyus* leaf extract with a utility in their antimicrobial interest. Since the antimicrobial impact of *Croton macrostachyus* had no activity through water extract, extraction through different solvents and reading its antimicrobial interest is needed. Commonly humans were using this plant as an antimicrobial agent in opposition to pathogens, however the usage of in extra may also have facet effects. Therefore, to pick out the dose-impact of this leaf extract extra study is encouraged.

## REFERENCES

1. Khan, I.; Saeed, K.; Khan, I. Nanoparticles : Properties, Applications and Toxicities. Arab. J. Chem. **2017**.
2. Khadeeja, P., Viktoria. B. and Lalita. L. Green synthesis of nanoparticles: Their advantages and disadvantages, 2nd Inter. Con. Techn: Micro to Nano **2015**, 1
3. Salunke, B.K., Prakash, K., Vishwakarma, and K.S., Maheshwari, V.L.: 'Plant metabolites: an alternative and sustainable approach towards post-harvest pest management in pulses', *Physiol. Mol. Biol. Plant.*, **2009**, 15, pp. 185–197.
4. Borase, H.P., Salunke, B.K., and Salunkhe, R.B.: 'Plant extract: a promising biomatrix for ecofriendly, controlled synthesis of silver nanoparticles', *Appl. Biochem. Biotechnol.*, **2014**, 173, 1–29.
5. Akintelu, S. A.; Folorunso, A. S.; Folorunso, F. A.; Oyebamiji, A. K. Green Synthesis of Copper Oxide Nanoparticles for Biomedical Application and Environmental Remediation. *Heliyon*, **2020**, 6 (7), 4508.
6. Narayanan, K. B; Sakthivel. N. Biological synthesis of metal nanoparticles by microbes. *Adva in Colloid and Interface Scie*, **2010**, 156, 1-13.
7. Duran, N; Marcato, P. D; Duran, M; Yadav, A; Gade, A. Rai. M. Mechanistic aspects in the biogenic synthesis of extracellular metal nanoparticles by peptides, bacteria, fungi and plants. *Appl Micr and Biote*, **2011**, 90, 1609-1624.
8. Kapingu, M. C; Guillaume, D; Mbwambo, Z. H; Moshi, M. J; Uliso, F. C; Mahunnah, R. L. Diterpenoids from the roots of *Croton macrostachys*. *Phytochemistry*, **2000**, 54(8), 767-770.
9. Käppeli, U; Hächler, H; Giezendanner, N; Beutin, L; Stephan. R. Human infections with non-O157 Shiga toxin-producing *Escherichia coli*, Switzerland, 2000-2009. *Emerg Infect Dis*. **2011**, 17(2), 180-185.
10. Karmali MA, Gannon V, Sargeant JM. Verocytotoxin- producing *Escherichia coli* (VTEC). *Vet Microbiol*. **2010**, 140(3-4), 360-370.
11. Kaur D, Jaiswal K, Mishra S. Ethnoveterinary Practices in India: A Review. *European Journal of Pharmaceutical and Medical Research*. **2015**, 2(7), 139-143.

12. Kelly BG, Vespermann A, Bolton DJ. The role of horizontal gene transfer in the evolution of selected foodborne bacterial pathogens. *Food Chem Toxicol.* **2009**, 47, 951-968.
13. Tolossa K, Debela E, Athanasiadou S, Tolera A, Ganga G, Houdijk J. Ethno-medicinal study of plants used for treatment of human and livestock ailments by traditional healers in South Omo, Southern Ethiopia. *J Ethnobiol Ethnomed.* **2013**, 9(1), 32.
14. Carlet J, Jarlier V, Harbarth S, Voss A, Goossens H, Pittet D. Ready for a world without antibiotics? The perspectives antibiotic resistance calls to action. *Antimicrob Resist Infect Control.* **2012**, 1, 11.
15. Khameneh B, Diab R, G 72. Khameneh B, Diab R, Ghazvini K, Bazzaz B. Breakthroughs in bacterial resistance mechanisms and the potential ways to combat them. *Microb Pathog.* **2016**, 95, 32-42.
16. Vineet, K., Kulvinder, S., Shaily, P. and Surinder, K.M. Green synthesis of manganese oxide nanoparticles for the electrochemical sensing of p-nitrophenol. *Int Nano Lett.* **2017**, 7, 123-131.
17. Reddy, R. N; Reddy, R. G. Synthesis and electrochemical characterization of amorphous MnO electrochemical capacitor electrode material. *J Power Sources*, **2004**, 132, 315-320.
18. Yuan, A; Wang, X; Wang, Y; Hu. J. Textural and capacitive characteristics of MnO nanocrystals derived from a novel solid-reaction route. *Electrochim Acta*, **2009**, 54, 1021-1026.
19. Zolfaghari, A; Ataherian, F; Ghaemi, M; Gholami. A. Capacitive behavior of nanostructured MnO prepared by sonochemistry method. *Electrochim Acta*, **2007**, 52, 2806-2814.
20. Kunkalekar. R.;K and Salker. A.;V. Low temperature carbon monoxide oxidation over nanosized silver doped manganese dioxide catalysts. *Catal Commun*, **2010**.12:193–196.
21. Salker, A.;V and Kunkalekar, R.;K. Palladium doped manganese dioxide catalysts for low temperature carbon monoxide oxidation. *Catal Commun*, **2009**. 10:1776–1780.
22. Dessie, Y.; Tadesse, S.; Eswaramoorthy, R. Physicochemical Parameter Influences and Their Optimization on the Biosynthesis of MnO<sub>2</sub> Nanoparticles Using Vernonia Amygdalina Leaf Extract. *Arab. J. Chem.* **2020**.

23. Moon, S. A.; Salunke, B. K.; Alkotaini, B.; Sathiyamoorthi, E. Plant Extract Biological Synthesis of Manganese Dioxide Nanoparticles by Kalopanax Pictus Plant Extract. *IET Nanobiotechnol* **2015**, Vol. 9, 220–225.
24. Krishnaraj, C.; Stacey, B. J.; Yun, L. H. S. Plant Extract-Mediated Biogenic Synthesis of Silver, Manganese Dioxide, Silver-Doped Manganese Dioxide Nanoparticles and Their Antibacterial Activity against Food- and Water-Borne Pathogens. *Bioprocess Biosyst. Eng.* **2016**.
25. Burda, C., Chen, X. B., Narayanan, R. and El-Sayed M. A. “Chemistry and properties of nanocrystals of different shapes”: *Chemical Reviews*. **2005**, vol. 105, no. 4, pp. 1025–1102.
26. Cao, J., Mao, Q. H., Shi, L. and Qian, Y. T. “Fabrication of  $\gamma$ -MnO<sub>2</sub>/ $\alpha$ -MnO<sub>2</sub>/ hollow core/shell structures and their application to water treatment”: *Journal of Matel. Chemistry*. **2011**, vol. 21, pp. 16210–16215.
27. Yan, D., Cheng, S. and Zhuo. R. F. “Nanoparticles and 3D sponge-like porous networks of manganese oxides and their microwave absorption properties,” *Nanotechnology*. **2009**, vol. 20, no.10, Article ID 105706.
28. Tan, Y. W., Meng, L. R., Peng, Q. and Li, Y.D. “One-dimensional single-crystalline Mn<sub>3</sub>O<sub>4</sub> nanostructures with tunable length and magnetic properties of Mn<sub>3</sub>O<sub>4</sub> nanowires,” *Chemical Communications*. **2011**, vol. 47, no. 4, pp. 1172–1174.
29. Zhang, X. Z. and Xing, Y. Yu et al., “Synthesis of Mn<sub>3</sub>O<sub>4</sub> nanowires and their transformation to LiMn<sub>2</sub>O<sub>4</sub> polyhedrons, application of LiMn<sub>2</sub>O<sub>4</sub> as a cathode in a lithium-ion battery,” *CrystEng- Comm*. **2012**, vol. 14, no. 4, pp. 1485–1489.
30. Ma, R., Bando, Y. Zhang, L. and Sasaki, T. “Layered MnO<sub>2</sub> nanobelts: hydrothermal synthesis and electrochemical measurement,” *Advanced Materials*. **2004**, vol. 16, no. 11, pp. 918–922.
31. Cheng, F. Y., Zhao, J. Z. and Song, W. et al., “Facile controlled synthesis of MnO<sub>2</sub> nanostructures of novel shapes and their application in batteries,” *Inorganic Chemistry*. **2006**, vol. 45, no. 5, pp. 2038–2044.
32. Cheng, F. Y., Shen, J. A., Peng, B., Pan, Y. D., Tao, Z. L. and Chen. J. “Rapid room-temperature synthesis of nanocrystalline spinels as oxygen reduction and evolution electrocatalysts,” *Nature Chemistry*. **2011**, vol. 3, pp. 79–84.

33. Sun, B., Chen, Z. X., Kim, H. S., Ahn, H. and Wang. G. X. "MnO/C core-shell nanorods as high capacity anode materials for lithium-ion batteries," *Journal of Power Sources*. **2011**, vol. 196, no.6, pp. 3346–3349.
34. Jaganyi, D., Altaf, M. and Wekesa. I. 'Synthesis and characterization of whisker-shaped MnO<sub>2</sub> nanostructure at room temperature'. *Appl. Nanosci.* **2013**, 3, pp. 329–333.
35. Wang, Y. and Xia. Y. Bottom-up and top-down approaches to the synthesis of monodispersed spherical colloids of low melting-point metals. *NanoLett.* **2004**, 4, 2047-2050.
36. Amechi, M. O. Green Synthesis of Silver Nanoparticles Using Leaf (. Green Synth. Silver Nanoparticles Using Leaf (Vernonia Amygdalina) Extr. Sel. Solvents its Charact. By Spectroscopic Methods Scanning Electron Microsc. **2018**.
37. Iravani, S. Green Synthesis of Metal Nanoparticles Using Plants Green Chemistry Green Synthesis of Metal Nanoparticles Using Plants. *Green Chem.* **2016**, 13, 2638–2650.
38. Links, D. A. Green Chemistry Green Synthesis of Metal Nanoparticles Using Plants. **2011**, 2638–2650.
39. Jadoun, S.; Arif, R.; Jangid, N. K.; Meena, R. K. Green Synthesis of Nanoparticles Using Plant Extracts: A Review. *Environ. Chem. Lett.* **2021**.
40. Chokriwal, A., Sharma, M. M., & Singh, A. (Biological synthesis of NPs using bacteria and their applications. *American Journal of PharmTech Research.* **2014**, 4, 39–61.
41. Moghaddam, A. B., Namvar, F., Moniri, M., Md.Tahir, P., Azizi, S., & Mohamad, R. Nanoparticles biosynthesized by fungi and yeast: A review of their preparation, properties, and medical applications. **2015**, *Molecules*, 20, 16540–16565.
42. Souri, M.; Hoseinpour, V.; Shakeri, A.; Ghaemi, N. Optimisation of Green Synthesis of MnO Nanoparticles via Utilising Response Surface Methodology. **2018**, 12, 822–827.
43. Nagajyothi, P. C.; Vattikuti, S. V. P.; Devarayapalli, K. C.; Yoo, K.; Sreekanth, T. V. M.; Vattikuti, S. V. P.; Devarayapalli, K. C.; Yoo, K. Technology Green Synthesis: Photocatalytic Degradation of Textile Dyes Using Metal and Metal Oxide Nanoparticles-Latest Trends and Advancements Green Synthesis: *Crit. Rev. Environ. Sci. Technol.*, **2019**, 0 (0), 1–107.

44. Palem, R. R.; Ganesh, S. D.; Kronekova, Z.; Sláviková, M.; Saha, N.; Saha, P. Green Synthesis of Silver Nanoparticles and Biopolymer Nanocomposites : A Comparative Study on Physico-Chemical , Antimicrobial and Anticancer Activity. *Bull. Mater. Sci.*, **2018**.
45. Yaqoob, A. A.; Ahmad, H.; Parveen, T.; Ahmad, A.; Oves, M. Recent Advances in Metal Decorated Nanomaterials and Their Various Biological Applications : A Review. **2020**, 8, 1–23.
46. Kunkalekar, R. K.; Prabhu, M. S.; Naik, M. M.; Salker, A. V. Colloids and Surfaces B : Biointerfaces Silver-Doped Manganese Dioxide and Trioxide Nanoparticles Inhibit Both Gram Positive and Gram Negative Pathogenic Bacteria. *Colloids Surfaces B Biointerfaces* **2014**, 113, 429–434.
47. Bai, B.; Qiao, Q.; Arandiyani, H.; Li, J.; Hao, J. Three-dimensional ordered mesoporous MnO<sub>2</sub> supported Ag nanoparticles for catalytic removal of formaldehyde. *Environ. Sci. Technol.* **2016**, 50, 2635–2640.
48. Kunkalekar, R.K.; Naik, M.M.; Dubey, S.K.; Salker, A.V. Antibacterial activity of silver-doped manganese dioxide nanoparticles on multidrug-resistant bacteria. *J Chem. Technol. Biotechnol.* **2012**, 88, 873–877.
49. Abu-dief, A. M. Development of Metal Oxide Nanoparticles as Semiconductors. **2020**, 1(1), 5–10.
50. Anandan, S.; Lee, G.; Wu, J. J. Ultrasonics Sonochemistry Sonochemical Synthesis of CuO Nanostructures with Different Morphology. *Ultrason. - Sonochemistry*, **2012**, 19 (3), 682–686.
51. Mobasser, S.; Akbar Firoozi, A. Review of Nanotechnology Applications in Science and Engineering. *J. homepage www.ojceu.ir J. Civ. Eng. Urban.*, **2016**, 6 (4), 84–93.
52. Krishnaiah D, Sarbatly and R, Bono A. Phytochemical antioxidants for health and medicine: A move towards nature. *Biotechnology Molecular Biology*. **2007**, 1: 97-104.
53. Carlet J, Jarlier V, Harbarth S, Voss and A, Goossens H, Pittet D. Ready for a world without antibiotics? The pensieres antibiotic resistance calls to action. *Antimicrob Resist Infect Control*. **2012**, 1: 11.
54. Burt S. Essential oils: their antibacterial properties and potential applications in foods: A review. *Int J Food Microbiol*. **2004**, 94:223-253.
55. Linscott AJ. Food-borne illnesses. *Clinical Microbiology Newsletter*.**2011**, 33(6): 41-45.

56. Baudot, C.; Ming, C.; Chien, J. Infrared Physics & Technology FTIR Spectroscopy as a Tool for Nano-Material Characterization. *Infrared Phys. Technol.*, **2010**, 53 (6), 434–438.
57. Press, D. One-Step Green Synthesis and Characterization of Leaf Extract-Mediated Biocompatible Silver and Gold Nanoparticles from *Memecylon Umbellatum*. **2013**, 1307–1315.
58. Birkholz, M. Thin Film Analysis by X-Ray Scattering; **2006**.
59. Bunaciu, A. A.; Udriștioiu, E.; Aboul-enein, H. Y.; Bunaciu, A. A.; Udriștioiu, E.; Aboul-enein, H. Y.; Bunaciu, A. A.; S, E. G. U. Critical Reviews in Analytical Chemistry X-Ray Diffraction : Instrumentation and Applications X-Ray Diffraction : Instrumentation and Applications. **2015**, 8347.
60. Jensen, H.; Pedersen, J. H.; J, J. E.; Pedersen, J. S.; Joensen, K. D.; Iversen, S. B.; S, E. G.; Pedersen, J. H.; J, J. E.; Pedersen, J. S. Determination of Size Distributions in Nanosized Powders by TEM , XRD , and SAXS. **2007**, 8080.
61. Sharma, S. K.; Verma, D. S.; Khan, L. U.; Kumar, S.; Khan, S. B. Handbook of Materials Characterization.
62. Liu, J. Scanning Transmission Electron Microscopy and Its Application to the Study of Nanoparticles and Nanoparticle Systems. *J. Electron Microsc.* (Tokyo)., **2005**, 54 (3).
63. Jayandran, M.; Haneefa, M. M.; Balasubramanian, V. Green Synthesis and Characterization of Manganese Nanoparticles Using Natural Plant Extracts and Its Evaluation of Antimicrobial Activity. *J. Appl. Pharm. Sci.* **2015**, Vol. 5 (12), 105-110.
64. Taye, B., Giday, M., Animut, A. and Seid. A. Antimicrobial activity of selected plants in traditional treatment of wounds in Ethiopia. *Asian Pacific Journal of Tropical Biomedical.* **2011**, 1, 370-375.
65. Teklehaymanot, T. and Giday. M. Ethnobotanical study of medicinal plants used by people in Zegie Peninsula, Northwestern Ethiopia. *J Ethnobiol Ethnomedicine.* **2007**, 3,12
66. Tenover, F.C., Biddle, J.W., Lancaster, M.V., Increasing resistance to vancomycin and other glycopeptides in *Staphylococcus aureus*. *Emerg Infect Dis.* **2001**, 7(2), 327-332.
67. Tenover FC. Mechanisms of antimicrobial resistance in bacteria. *Am J Infect Control.* **2006**; 34(5 Suppl 1): S3-S10.



68. Tolossa, K., Debela, E., Athanasiadou, S., Tolera, A., Ganga, G. and Houdijk, J. Ethno-medicinal study of plants used for treatment of human and livestock ailments by traditional healers in South Omo, Southern Ethiopia. *J Ethnobiol Ethnomed.* **2013**, 9(1), 32
69. Tewelde, S. and Ghebriel. O. Phytochemical investigation and antimicrobial activities of the fruit extract of *Solanum incanum* grown in Eretria. *Ornamental and Medicinal Plants.* **2017**, 1(1), 15-25.
70. Tiwari, P., Kumar, B., Kaur, M., Kaur, G. and Kaur. H. Phytochemical screening and extraction: A Review. *Internationale Pharmaceutica Scientia.* **2011**, 1, 98-106.
71. López-Campos, G., Martínez-Suárez, J., Aguado-Urda, M. and López-Alonso. V. Detection, identification, and analysis of foodborne pathogens. In: *Microarray Detection and Characterization of Bacterial Foodborne Pathogens.* Boston, MA, USA: Springer Publisher. **2012**, 13-32
72. Maroyi, A. Ethnopharmacological uses, phytochemistry, and pharmacological properties of *Croton macrostachyus* Hochst. Ex Delile: A comprehensive review. *Evid-Based Compl. and Alter. Medi.* **2017**, 1-17
73. Matu, E.N. *Solanum incanum* L. *Plant Resources of Tropical Africa.* **2008**, 2(1), 525-528.
74. McEvoy, J. M., Doherty, A. M. and Sheridan. J.J. The prevalence and spread of *Escherichia coli* O157:H7 at a commercial beef abattoir. *J Appl Microbiol.* **2003**, 95(2), 256-266.
75. Mechesso, A., Tadese, A., Tesfaye, R., Tamiru, W. and Eguale. T. Experimental evaluation of wound healing activity of *Croton macrostachyus* in rat. *African Journal of Pharm. and Pharmacology.* **2016**, 10(39), 832-838.
76. Abdisa, T. Medicinal Value of *Croton Macrostachyus* and *Solanum Incanum* against Causative Agent of Foodborne Diseases. *Vet. Med.* **2019**, 4 (2), 57–68.
77. Mekonnen, L. B. In Vivo Antimalarial Activity of the Crude Root and Fruit Extracts of *Croton Macrostachyus* (Euphorbiaceae) against *Plasmodium Berghei* in Mice. *J. Tradit. Complement. Med.* **2015**, 5 (3), 168–173.
78. Jones, W. P.; Kinghorn, A. D. Chapter 13 Extraction of Plant Secondary Metabolites. *Satyajit D. Sarker Lutfun Nahar (eds.), Nat. Prod. Isol. Methods Mol. Biol.* **864**, 341–366.
79. Reviewed, P. Green Synthesis of Manganese Oxide Nanoparticles Using. **2021**, 514 (4), 112–117.

80. Moorthy, S. K.; Ashok, C. H.; Rao, K. V.; Viswanathan, C. MgONanoparticles by Neem Leaves Through Green Method. *Mater. Today Proc.* **2015**, 2 (9), 4360–4368.
81. Sakthi, Dr. G. and Saravanakumari .Dr. P.” Green synthesis of manganese oxide nanoparticles”, Peer Reviewed and Refereed Journal, **2021**, vol 10, ISSUE:4 (7).
82. Ahmed, M. U.; Dahiru, J. N.; Sudi, I. Y.; Gabriel, S.; John, I. K. Asian Journal of Applied Sciences Green Synthesis of Manganese Oxide Nanoparticles from Cassia Tora Leaves and Its Toxicological Evaluation. *Asian J. Appl. Sci.* **2020**, 13, 60–67.
83. Kumar, V. Green Synthesis of Manganese Oxide Nanoparticles for the Electrochemical Sensing of p -Nitrophenol. *Int. Nano Lett.* **2017**.
84. Hoseinpour, V.; Sourı, M.; Ghaemi, N.; Shakeri, A.; Vi, I. I. Optimization of Green Synthesis of ZnO Nanoparticles by Dittrichia Graveolens ( L .) Aqueous Extract. **2017**, 1, 39–49.
85. Sourı, M.; Hoseinpour, V.; Ghaemi, N.; Shakeri, A. Procedure Optimization for Green Synthesis of Manganese Dioxide Nanoparticles by Yucca Gloriosa Leaf Extract. *Int. Nano Lett.* **2019**, 9 (1), 73–81.
86. Ogunyemi, S. O.; Zhang, F.; Abdallah, Y.; Zhang, M.; Wang, Y.; Sun, G.; Qiu, W.; Li, B. Biosynthesis and Characterization of MgO & MnO<sub>2</sub> Nanoparticles Using Matricaria Chamomilla L. Extract and Its Inhibitory Effect on Acidovorax Oryzae Strain RS-2. *Artif. Cells, Nanomedicine Biotechnol.* **2019**, 47 (1), 2230–2239.
87. Shakeel, A, K.; Sammia, Sh. Basma, Sh. U. F.; Saddam, A.; A. Green Synthesis of MnO NPs Using Abutilon Indicum Leaf Extract for Biological, *Biomolecules* **2020**. 10, 785.
88. Chatterjee, S.; Anita, J.; Subramanian, A.; Subramanian, S. Synthesis and Characterization of Manganese Dioxide Using Brassica Oleracea ( Cabbage ). **2017**, 33 (2), 1627–1632.
89. Ciorîță, A.; Suci, M.; Macavei, S.; Kacso, I.; Lung, I.; Soran, M. L.; Pârvu, M. Green Synthesis of Ag-MnO<sub>2</sub> Nanoparticles Using Chelidonium Majus and Vinca Minor Extracts and Their in Vitro Cytotoxicity. *Molecules* **2020**, 25 (4).
90. Widyaningtyas, A. L.; Yulizar, Y.; Bagus, D. O. Ag<sub>2</sub>O Nanoparticles Fabrication by Vernonia Amygdalina Del. Leaf Extract: Synthesis, Characterization, and Its Photocatalytic Activities, I. *Mater. Sci. Eng. Pap.* **2019**, No. 012022.
91. Alshareef, H. N.; Chen, W.; Rakhi, R. B.; Hu, L.; Xie, X.; Cui, Y. High Performance Nanostructured Supercapacitors on a Sponge. *Nano Lett.* **2011**, 11, 5165–5172.
92. Kunkalekar, R. K.; Prabhu, M. S.; Naik, M. M.; Salker, A. V. Silver-Doped Manganese Dioxide and Trioxide Nanoparticles Inhibit Both Gram Positive and Gram Negative Pathogenic Bacteria. *Colloids Surfaces B Biointerfaces* **2014**, 113, 429–434.

APPENDIXES



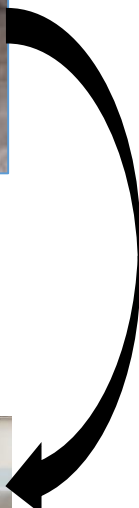
**A**  
*C. macrostachyus* leaf



**B**  
dried *C. macrostachyus* leaf



**C**  
Grinding



**F**  
Crude extract at 4°C stored

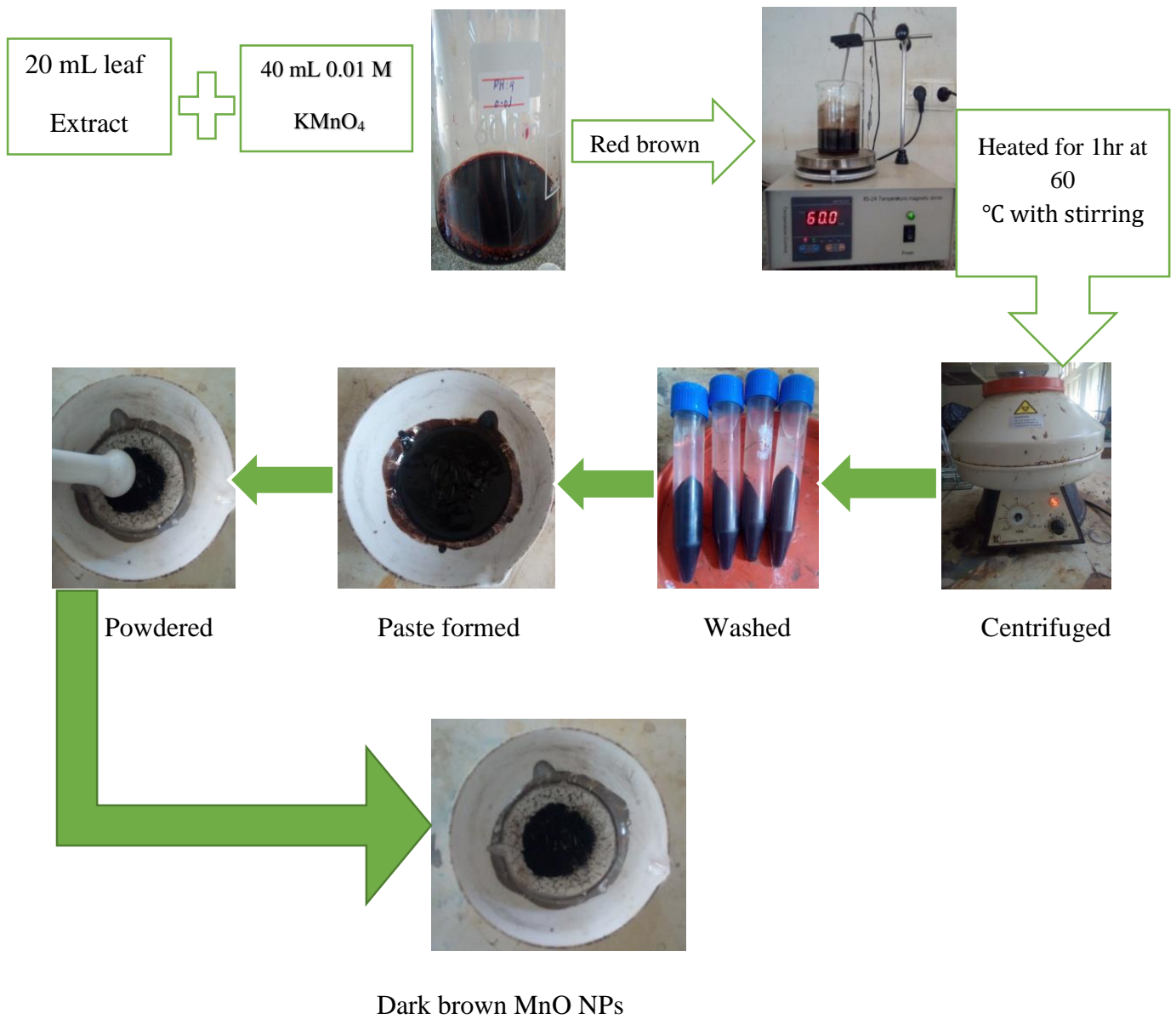


**E**  
Filtration process

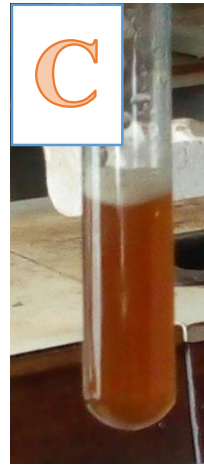
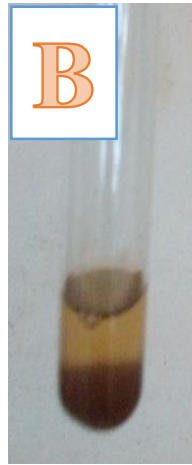


**D**  
Hot with magnetic stirrer

**Appendix 1** schematic diagram show the preparation of *croton macrostachyus* leaf extract.



**Appendix 2** Schematic diagram show the formation of manganese oxide nanoparticles.



**Appendix 3** Phytochemical screening of phenols, flavonoids and alkaloids.